Complete classification of spherically symmetric self-similar perfect fluid solutions

B. J. Carr
Astronomy Unit, Queen Mary & Westfield College, Mile End Road, London E1 4NS, England

A. A. Coley
Department of Mathematics & Statistics, Dalhousie University, Halifax, Nova Scotia, Canada B3H 3J5
(Received 4 March 1998; revised manuscript received 23 December 1999; published 24 July 2000)

We classify all spherically symmetric perfect fluid solutions of Einstein's equations with an equation of state $p=\alpha\mu$ which are self-similar in the sense that all dimensionless variables depend only upon $z\equiv r/t$. This extends a previous analysis of dust ($\alpha=0$) solutions. Our classification is ''complete'' subject to the restrictions that α lies in the range 0 to 1 and that the solutions are everywhere physical and shock-free. For a given value of α, such solutions are described by two parameters and they can be classified in terms of their behavior at large and small distances from the origin; this usually corresponds to large and small values of $|z|$ but (due to a coordinate anomaly) it may also correspond to finite z. We base our analysis on the demonstration (given elsewhere) that all self-similar solutions must be asymptotic to solutions which depend on either powers of z at large and small $|z|$ or powers of $\ln|z|$ at finite z. We show that there are only three self-similar solutions which have an *exact* power-law dependence on z: the flat Friedmann solution, a static solution and a Kantowski-Sachs solution (although this is probably only physical for $\alpha<-1/3$). At large values of $|z|$, we show that there is a 1-parameter family of asymptotically Friedmann solutions, a 1-parameter family of asymptotically Kantowski-Sachs solutions and a 2-parameter family which we describe as asymptotically ''quasi-static.'' For $\alpha>1/5$, there are also two families of asymptotically Minkowski solutions at large distances from the origin, although these do not contain the Minkowski solution itself: the first is asymptotical to the Minkowski solution as $|z|\to\infty$ and is described by one parameter; the second is asymptotical to the Minkowski solution at a finite value of z and is described by two parameters. The possible behaviors at small distances from the origin depend upon whether or not the solutions pass through a sonic point. If the solutions remain supersonic everywhere, the origin corresponds to either a black hole singularity or a naked singularity at finite z. However, if the solutions pass into the subsonic region, their form is restricted by the requirement that they be ''regular'' at the sonic point and any physical solutions must reach $z=0$. As $z\to 0$, there is again a 1-parameter family of asymptotic Friedmann solutions: this includes a continuum of underdense solutions and discrete bands of overdense ones; the latter are all nearly static close to the sonic point and exhibit oscillations. There is also a 1-parameter family of asymptotically Kantowski-Sachs solutions but no asymptotically static solutions besides the exact static solution itself. The full family of solutions can be found by combining the possible large and small distance behaviors. We discuss the physical significance of these solutions.

PACS number(s): 04.20.Jb, 95.30.Sf, 98.80.Hw

I. INTRODUCTION

Self-similar models have proved very useful in general relativity because the similarity assumption reduces the complexity of the partial differential equations. Even greater simplification is achieved if one has spherical symmetry [1] since the governing equations then reduce to comparatively simple ordinary differential equations. In this case, the solutions can be put into a form in which every dimensionless variable is a function of some dimensionless combination of the cosmic time coordinate t and the comoving radial coordinate r. In the simplest situation, a self-similar solution is invariant under the transformation $r\to ar, t\to at$ for any constant a and the similarity variable is $z=r/t$. Geometrically this corresponds to the existence of a homothetic Killing vector and is sometimes termed self-similarity of the ''first'' kind. We confine attention to such solutions in this paper. We shall also focus on the case in which the source of the gravitational field is a perfect fluid with an equation of state of the form $p=\alpha\mu$. Indeed, one can show that this is the only barotropic equation of state compatible with the similarity assumption [1]. We will assume $|\alpha|\leqslant 1$, as required by causality, and usually take α to be positive. We will also assume that α is the same everywhere. Note that ''geometric'' self-similarity (a property of the metric) and ''physical'' self-similarity (a property of the fluid) coincide for a perfect fluid but this need not be the case in general [2].

What makes such solutions of more than mathematical interest is the fact that they are often relevant to the real world [3]. For example, an explosion in a homogeneous background produces fluctuations which may be very complicated initially but which tend to be described more and more closely by a spherically symmetric self-similar solution as time evolves [4]. This applies even if the explosion occurs in an expanding cosmological background [5]. The evolution of cosmic voids may also be described by a self-similar solution at late times [6]. A gravitationally bound cloud collapsing from an initially static configuration may evolve to self-similar form [7] and recently it has become clear that spherically symmetric self-similar solutions play a crucial

role in the context of ''critical'' phenomena [8–10]. Such considerations led Carr [11] to propose the ''similarity hypothesis,'' which postulates that under certain circumstances spherically symmetric solutions may naturally evolve to a self-similar form even if they start out more complicated. It is well known that self-similar solutions play a crucial asymptotic role in the context of spatially homogenous models [12], so this extends that result.

The possibility that self-similar models may be singled out in this way from more general spherically symmetric solutions means that it is essential to understand the full family of such solutions. A complete classification of self-similar dust ($\alpha=0$) solutions has already been provided [13] and the purpose of the present paper is to extend this classification to a perfect fluid with pressure ($\alpha\neq 0$). We will show that some of the features of the dust solutions carry over to the more general case but by no means all of them. Indeed some of the solutions with pressure have no analogue at all in the dust case. The extra complications arise because solutions with pressure generally have a shock [1] or sonic point [14] and the nature of the discontinuity at this point plays a crucial role. However, a full understanding of these effects has only come rather recently. In this paper we will only consider solutions with sound-waves and we will focus exclusively on solutions which are ''regular'' at the sonic point in the sense that they have a finite pressure gradient and can be continued beyond there. Even some of these solutions will turn out to be unphysical, in the sense that they encounter either another (irregular) sonic point or a domain where the mass is negative.

Due to the existence of several preferred geometric structures in self-similar spherically symmetric models, a number of natural approaches (i.e. coordinate systems) may be used in studying them [15]. The three most common ones are the ''comoving,'' ''homothetic'' and ''Schwarzschild'' approaches. In the comoving approach, pioneered by Cahill and Taub [1] and employed by Carr and Henriksen and co-workers, the coordinates are adapted to the fluid 4-velocity vector. This probably affords the best physical insights and is the most convenient one with which to study the solutions explicitly. In the homothetic approach, used by Bogoyavlenski and co-workers, and adopted more recently by Brady [16] and Goliath et al. [17,18], the coordinates are adapted to the homothetic vector. In this case, the governing equations reduce to those of an autonomous system and so dynamical systems theory can be exploited to study the equations mathematically. The ''Schwarzschild'' approach, adopted by Ori and Piran [19] and Maison [9], is useful if one wishes to match a self-similar interior region to a non-self-similar asymptotically flat exterior region. This is because one can analyze null geodesics most simply in these coordinates, enabling the causal structure of spacetime to be studied. The relationship between these different approaches is discussed in more detail in Appendix A. All of them are complementary and which is most suitable depends on what type of problem one is studying. In this paper it is most convenient to use the comoving approach.

The first step in providing a complete classification of perfect fluid spherically symmetric self-similar solutions is to analyze all possible behaviors at large and small distances from the origin. In the simplest situation this just corresponds to large and small values of the similarity variable $z=r/t$ but the analysis is complicated by the fact that (due to a coordinate anomaly) a finite value of z may sometimes correspond to zero or infinite distance from the origin. A rigorous demonstration that our asymptotic classification is complete is given elsewhere [20] and consists of two parts: (1) an analysis of all solutions whose asymptotic behavior is associated with large or small values of $|z|$ and a demonstration that these always have a power-law dependence on z; (2) an analysis of solutions whose asymptotic behavior is associated with a *finite* value of z and a demonstration that these have a power-law dependence on $\ln|z|$. We use this ''power-law'' property as the starting point of the analysis in the present paper. This shortens the discussion considerably and allows us to focus on the nature and physical significance of the solutions.

We will show that perfect fluid self-similar spherically symmetric solutions have four possible behaviors at large distances from the origin. They are either asymptotically Friedmann, asymptotically ''quasi-static,'' asymptotically Kantowski-Sachs or asymptotically Minkowski, with the last family being subdivided into two (one of which is associated with a finite value of z). The possible behaviors at small distances depend upon whether or not the solutions pass through a sonic point. If the solutions remain supersonic everywhere, the origin is at finite z and corresponds to either a black hole singularity or a naked singularity; in either case, the small-$|z|$ behavior is uniquely determined by the large-$|z|$ behavior. If the solutions pass through a sonic point, they may be discontinuous there and the situation is more complicated. However, in this paper we confine attention to solutions which are regular at the sonic point and physically realistic throughout the subsonic regime. All such solutions reach $z=0$ and have three possible behaviors at small $|z|$: they are either asymptotically Friedmann, exactly static or asymptotically Kantowski-Sachs. If the solutions are required to be analytic at the sonic point, then they are still determined uniquely by the large-scale behavior. If they are merely required to be C^1, the small and large $|z|$ behaviors must be specified independently. Not all supersonic solutions can be attached to $z=0$ via a sonic point; the ones which cannot either encounter a shock or become unphysical in some domain.

The complete family of solutions can be found by combining the four types of large-distance behaviors and the four types of small-distance behaviors. However, the Kantowski-Sachs solutions can only link to each other, so this yields ten different types of solution. It is useful to classify these solutions by their large-distance behavior. Since some of these solutions have been found before (see [21–23] for recent reviews), our discussion will necessarily involve some overview of previous work. However, this is the first time all the solutions have been brought together, with the connection between them being made explicit. It should be stressed that this work complements the dynamical systems analysis of Goliath et al. [17,18], which also delineates the different types of solutions but in a different way and without making

their physical significance clear. The precise relationship between our two approaches and a more detailed description of some of the solutions can be found elsewhere [10]. Since some of the discussion in this paper is rather technical, it will be useful to start off with a brief qualitative description of the various solutions and to relate them to the solutions found by earlier workers.

The first class of solutions is a 1-parameter family asymptotic to the flat Friedmann solution at large values of $|z|$. The solutions with $z>0$ can be regarded as inhomogeneous big bang models which expand from an initial singularity at $z=\infty$ and then either expand indefinitely or recollapse to a black hole as z decreases. Attention originally focussed on models containing black holes because there was interest in whether black holes could grow at the same rate as the particle horizon. Carr and Hawking [24] showed that such solutions exist for radiation ($\alpha=1/3$) and dust ($\alpha=0$) but only if the universe is asymptotically rather than exactly Friedmann (i.e. there is no solution in which a black hole interior is attached to an exact Friedmann exterior via a sound-wave) and this has the important implication that black holes formed through purely local processes cannot grow as fast as the Universe. Carr [25] and Bicknell and Henriksen [26] then extended this result to a general $0<\alpha<1$ fluid, while Lin et al. [27] and Bicknell and Henriksen [28] considered the case of a stiff fluid ($\alpha=1$). The ever-expanding solutions can be interpreted as density fluctuations in a flat Friedmann model which grow at the same rate as the Universe [29]. These solutions are asymptotical to the Friedmann solution at both large and small values of $|z|$ and regular at the sonic point. Such transonic solutions can be either underdense or overdense relative to the exact Friedmann model. There is a continuum of regular underdense solutions and these may be relevant to the existence of large-scale cosmic voids [30]. Regular overdense solutions may only occur in very narrow bands; these have the characteristic that they are all approximately static near the sonic point, although they depart from the static solution and exhibit oscillations as they approach the origin.

The second class of models is associated with the Kantowski-Sachs solution. This is a type of homogeneous model first studied by Kantowski and Sachs [31] for the $\alpha=0$ case and then by Collins [32] for arbitrary α. For each α there is a unique self-similar Kantowski-Sachs solution and there also exists a 1-parameter family of solutions asymptotic to this at both large and small values of $|z|$ [33]. Solutions with $-1/3<\alpha<1$ are probably unphysical because the mass is negative and they are also tachyonic for $0<\alpha<1$. Solutions with $-1<\alpha<-1/3$ avoid these unsatisfactory features. Although such equations of state violate the strong energy condition, they could could well arise in the early Universe due to inflation or particle production effects. Such models may be related to the growth of $p>0$ bubbles formed at a phase transition in a $p<0$ cosmological background [34]. Note that this is the only context in which we will consider negative values of α.

The third class of models are related to the self-similar static model. There is just one exactly static self-similar solution for each (positive) value of α [35] and there is a 1-parameter family of solutions asymptotic to this at large values of $|z|$. However, we will show that there is also a 2-parameter family of solutions which are asymptotically ''quasi-static'' in the sense that they have an isothermal density profile at large values of $|z|$. Such solutions exist even in the dust case, although there is then no *exact* static solution [13]. A crucial feature of these solutions is that each one may span both positive and negative values of z, whereas each solution of the other types is confined to either positive or negative z. Such solutions can be regarded as inhomogeneous big bang models in which the initial or final singularity occurs at a finite (rather than infinite) value of z. Some of them expand or collapse monotonically; these necessarily have a sonic point and may be attached to an asymptotically Friedmann solutions in the subsonic regime. Others expand and then recollapse; these remain supersonic everywhere and contain two singularities at finite z, one of which may be naked. Some asymptotically quasi-static solutions have been studied before [19,36]. In particular, they may be associated with the occurrence of naked singularities [37] and the transonic ones are also associated with critical phenomena for $\alpha<0.28$ [10]. However, the precise relationship of these solutions to the more general quasi-static family has not been discussed before.

The fourth class of solutions, which only exist for $\alpha>1/5$, are asymptotically Minkowski and have not been previously analyzed at all. They were originally found numerically by Goliath et al. [18] and this led us to ''predict'' them analytically. There are actually two such families and they are described in more detail elsewhere [10]. Members of the first family are described by one parameter and are asymptotically Minkowski as $|z|\to\infty$; members of the second family are described by two parameters and are asymptotically Minkowski as z tends to some finite value (though this corresponds to an infinite physical distance unless $\alpha=1$). As with the asymptotically Friedmann and asymptotically quasi-static solutions, these may be either supersonic everywhere (in which case they contain a black hole or naked singularity) or attached to $z=0$ via a sonic point (in which case they are asymptotically Friedmann or exactly static at small $|z|$). The transonic ones are associated with critical phenomena for $\alpha>0.28$ [10].

The plan of this paper is as follows. In Sec. II we will introduce the relevant equations and discuss the crucial role of the sonic point. In Sec. III we will analyze the possible behaviors at large and small distances from the origin, emphasizing the key role played by the power-law and log-power-law solutions. In Sec. IV we will describe the full family of solutions, with special emphasis on those asymptotic to the Friedmann, Kantowski-Sachs and static solutions. We will show that many of their features in the supersonic regime can be understood by using the insights gained from the dust solutions, although some of the solutions have no analogue in the dust case. We make some final remarks in Sec. VI, qualifying the sense in which our classification is ''complete.'' Some technical issues are covered in the Appendixes.

II. SPHERICALLY SYMMETRIC SIMILARITY SOLUTIONS

In the spherically symmetric situation one can introduce a time coordinate t such that surfaces of constant t are orthogonal to fluid flow lines and comoving coordinates (r,θ,ϕ) which are constant along each flow line. The metric can then be written in the form

$$ds^2=e^{2\nu}\,dt^2-e^{2\lambda}\,dr^2-R^2\,d\Omega^2,\quad d\Omega^2\equiv d\theta^2+\sin^2\theta\,d\phi^2 \tag{2.1}$$

where ν, λ and R are functions of r and t. For a perfect fluid the Einstein equations are

$$G^{\mu\nu}=8\pi[(\mu+p)U^\mu U^\nu-p\,g^{\mu\nu}] \tag{2.2}$$

where $\mu(r,t)$ is the energy density, $p(r,t)$ the pressure, $U^\mu=(e^{-\nu},0,0,0)$ is the comoving fluid 4-velocity, and we choose units in which $c=G=1$. The equations have a first integral

$$m(r,t)=\tfrac{1}{2}R\left[1+e^{-2\nu}\left(\frac{\partial R}{\partial t}\right)^2-e^{-2\lambda}\left(\frac{\partial R}{\partial r}\right)^2\right] \tag{2.3}$$

and this can be interpreted as the mass within comoving radius r at time t:

$$m(r,t)=4\pi\int_0^r \mu R^2\frac{\partial R}{\partial r'}\,dr'. \tag{2.4}$$

Unless $p=0$, this quantity decreases with increasing t because of the work done by the pressure. One can also express it as

$$m(r,t)=4\pi\int_0^t pR^2\frac{\partial R}{\partial t'}\,dt' \tag{2.5}$$

and this is the more appropriate expression when there is no spatial origin (as in the Kantowski-Sachs solution). Eq. (2.3) can be written as an equation for the energy per unit mass of the shell with comoving coordinate r:

$$\mathcal{E}\equiv\frac{1}{2}U^2-\frac{m}{R},\quad U\equiv e^{-\nu}\left(\frac{\partial R}{\partial t}\right). \tag{2.6}$$

This can be interpreted as the sum of the kinetic and potential energies per unit mass. Only in the $p=0$ case is $\mathcal{E}$ conserved along fluid flow lines.

By a spherically symmetric self-similar solution we shall mean one in which the spacetime admits a homothetic Killing vector $\boldsymbol{\xi}$ that satisfies

$$\xi_{\mu;\nu}+\xi_{\nu;\mu}=2g_{\mu\nu}. \tag{2.7}$$

This means that the solution is unchanged by a transformation of the form $t\to at$, $r\to ar$ for any constant a. Solutions of this sort were first investigated by Cahill and Taub [1], who showed that by a suitable coordinate transformation they can be put into a form in which all dimensionless quantities such as ν, λ, $\mathcal{E}$ and

$$S\equiv\frac{R}{r},\quad M\equiv\frac{m}{R},\quad P\equiv pR^2,\quad W\equiv\mu R^2 \tag{2.8}$$

are functions only of the dimensionless variable $z\equiv r/t$. Then we have

$$\frac{\partial}{\partial t}=-\frac{z^2}{r}\frac{d}{dz},\quad \frac{\partial}{\partial r}=\frac{z}{r}\frac{d}{dz}, \tag{2.9}$$

so the field equations reduce to a set of ordinary differential equations in z. Another important quantity is the function

$$V(z)=e^{\lambda-\nu}z, \tag{2.10}$$

which represents the velocity of the surfaces of constant z relative to the fluid. These surfaces have the equation $r=zt$ and therefore represent a family of spheres moving through the fluid. The spheres contract relative to the fluid for $z<0$ and expand for $z>0$. This is to be distinguished from the velocity of the spheres of constant R relative to the fluid:

$$V_R=-e^{\lambda-\nu}\left(\frac{\partial R/\partial t}{\partial R/\partial r}\right). \tag{2.11}$$

This is positive if the fluid is collapsing and negative if it is expanding. Special significance is attached to values of z for which $|V|=1$ and $|V_R|=1$. The first corresponds to a Cauchy horizon (either a black hole event horizon or a cosmological particle horizon), the second to a black hole or cosmological apparent horizon. We show shortly that the existence of an apparent horizon is also equivalent to the condition $M=1/2$.

The only barotropic equation of state compatible with the similarity ansatz is one of the form $p=\alpha\mu$ $(-1\leqslant\alpha\leqslant 1)$. As discussed by Carr and Yahil [29], whose analysis we now follow, it is convenient to introduce a dimensionless function $x(z)$ defined by

$$x(z)\equiv(4\pi\mu r^2)^{-\alpha/(1+\alpha)}. \tag{2.12}$$

[Note that the factor of 4π is omitted in the definition of x given by Carr and Yahil but it is required for consistency with eq. (2.3).] The conservation equations $T^{\mu\nu}{}_{;\nu}=0$ can then be integrated to give

$$e^{\nu}=\beta x z^{2\alpha/(1+\alpha)}, \tag{2.13}$$

$$e^{-\lambda}=\gamma x^{-1/\alpha}S^2, \tag{2.14}$$

where β and γ are integration constants. The remaining field equations reduce to a set of ordinary differential equations in x and S:

$$\ddot{S}+\dot{S}+\left(\frac{2}{1+\alpha}\frac{\dot{S}}{S}-\frac{1}{\alpha}\frac{\dot{x}}{x}\right)[S+(1+\alpha)\dot{S}]=0, \tag{2.15}$$

$$\left(\frac{2\alpha\gamma^2}{1+\alpha}\right)S^4+\frac{2}{\beta^2}\frac{\dot{S}}{S}x^{(2-2\alpha)/\alpha}z^{(2-2\alpha)/(1+\alpha)}-\gamma^2S^4\frac{\dot{x}}{x}\left(\frac{V^2}{\alpha}-1\right)$$
$$=(1+\alpha)x^{(1-\alpha)/\alpha}, \tag{2.16}$$

$$M = S^2 x^{-(1+\alpha)/\alpha}\left[1+(1+\alpha)\frac{\dot{S}}{S}\right], \tag{2.17}$$

$$M = \frac{1}{2} + \frac{1}{2\beta^2} x^{-2} z^{2(1-\alpha)/(1+\alpha)} \dot{S}^2 - \frac{1}{2}\gamma^2 x^{-(2/\alpha)} S^6 \left(1+\frac{\dot{S}}{S}\right)^2, \tag{2.18}$$

where the velocity function is given by

$$V = (\beta\gamma)^{-1} x^{(1-\alpha)/\alpha} S^{-2} z^{(1-\alpha)/(1+\alpha)} \tag{2.19}$$

and an overdot denotes $z\,d/dz$. The other velocity function is

$$V_R = \frac{V\dot{S}}{S+\dot{S}}, \tag{2.20}$$

while the energy function is

$$\mathcal{E} = \frac{1}{2}\gamma^2 x^{-(2/\alpha)} S^6 \left(1+\frac{\dot{S}}{S}\right)^2 - \frac{1}{2} \tag{2.21}$$

and this always exceeds $-1/2$. Equation (2.18) can then be written in the form

$$M = \frac{1}{2} + \left(\mathcal{E}+\frac{1}{2}\right)(V_R^2 - 1), \tag{2.22}$$

so the condition $M=1/2$ is equivalent to the condition $|V_R|=1$ (corresponding to an apparent horizon). The special case $\mathcal{E}=-1/2$ corresponds to the Kantowski-Sachs solution, for which V_R diverges and $M \neq 1/2$.

We can best envisage how these equations generate solutions by working in the 3-dimensional $(x,S,\dot{S})$ space [29]. At any point in this space, for a fixed value of α, Eqs. (2.17) and (2.18) give the value of z; Eq. (2.16) then gives the value of $\dot{x}$ unless $|V|=\sqrt{\alpha}$ and Eq. (2.15) gives the value of $\ddot{S}$. Thus the equations generate a vector field $(\dot{x},\dot{S},\ddot{S})$ and this specifies an integral curve at each point of the 3-dimensional space. Each curve is parametrized by z and represents one particular similarity solution. This shows that, for a given equation of state parameter α, there is a 2-parameter family of spherically symmetric self-similar solutions.

In $(x,S,\dot{S})$ space the sonic condition $V=\sqrt{\alpha}$ specifies a 2-dimensional surface because Eqs. (2.17) to (2.19) allow one to express $\dot{S}$ in terms of x and S. The same surface corresponds to the condition $V=-\sqrt{\alpha}$. Where a curve intersects this surface, Eq. (2.16) does not uniquely determine $\dot{x}$, so there can be a number of different solutions passing through the same point. However, integral curves intersect $|V|=\sqrt{\alpha}$ in a physically reasonable manner only if

$$\left(\frac{2\alpha\gamma^2}{1+\alpha}\right)S^4 + \frac{2}{\beta^2}\frac{\dot{S}}{S} x^{(2-2\alpha)/\alpha} z^{(2-2\alpha)/(1+\alpha)} = (1+\alpha)x^{(1-\alpha)/\alpha}, \tag{2.23}$$

since otherwise the value of $\dot{x}$ and hence the pressure, density and velocity gradient diverge there. Since Eq. (2.23) corresponds to another 2-dimensional surface in $(x,S,\dot{S})$ space, this will intersect the surface $|V|=\sqrt{\alpha}$ on a line Q. Only integral curves which hit the sonic surface on this line are ''regular'' in the sense that they can be extended beyond there. (All other solutions would have to contain shock-waves.) From each point on this line there will be regular integral curves with decreasing and increasing z. One can join any member of the first kind to any member of the second kind to obtain a complete self-similar solution.

Physically reasonable solutions cannot have an arbitrary value of $\dot{x}$ at $|V|=\sqrt{\alpha}$. If we require $\ddot{x}$ to be finite there, then the equations permit just two values of $\dot{x}$ at each point of the line Q and there will then be two corresponding values of $\dot{V}$. If these values are complex, corresponding to a *focal* point, then the solutions will spiral around the sonic point and be unphysical. If they are real, at least one of the values of $\dot{V}$ must be positive. If both values of $\dot{V}$ are positive, corresponding to a *nodal* point, then the smaller ''primary'' one is associated with a 1-parameter family of solutions, while the larger ''secondary'' one is associated with an isolated solution. If one of the values of $\dot{V}$ is negative, corresponding to a *saddle* point, then both values are associated with isolated solutions. This behavior has been analyzed in detail by several authors [14,19,28,29].

One can show that there is a 1-parameter family of regular solutions (i.e. a node) only on a restricted part of the line Q and, in the $V(z)$ diagram, this corresponds to two ranges of values for $|z|$. For positive z, one range $(z_1<z<z_2)$ lies to the left of the Friedmann sonic point z_F and includes the static sonic point z_S; the other goes from some value z_3 to infinity and includes z_F. There is a saddle point for $z<z_1$ and a focal point for $z_2<z<z_3$. These features are indicated in Fig. 1(a). The values of z_1, z_2 and z_3 can be expressed in terms of α but the expressions are complicated, so we do not give them explicitly. The ranges for $\alpha=1/3$ are indicated in Fig. 1(b); in this case, $z_3=z_F$ and $z_2=z_S$. Generally one has $z_2<z_S<z_3$ and $z_F>z_3$.

We will argue later that any solutions described by just one parameter asymptotically (and this includes all the solutions from $z=0$) must hit the sonic line in the nodal ranges and these will be physical only for certain bands of parameters. On each side of the node, $\dot{V}$ may have either of its two possible values. If one chooses different values for $\dot{V}$, there will be a discontinuity in the pressure gradient, so the solution will be C^0. If one chooses the same value, there may still be a discontinuity in the second derivative of V, in which case the solution will be C^1. Only the isolated solution and a single member of the 1-parameter family of solutions at each node are analytic. Solutions described by two parameters at large $|z|$ may also hit the sonic line in the saddle range. These would necessarily be analytic at the sonic point but not generally physical in the subsonic region. In the case of a shock V would itself be discontinuous.

III. ASYMPTOTIC BEHAVIOR OF SELF-SIMILAR SOLUTIONS

The key step in providing a complete classification of spherically symmetric perfect fluid self-similar solutions is

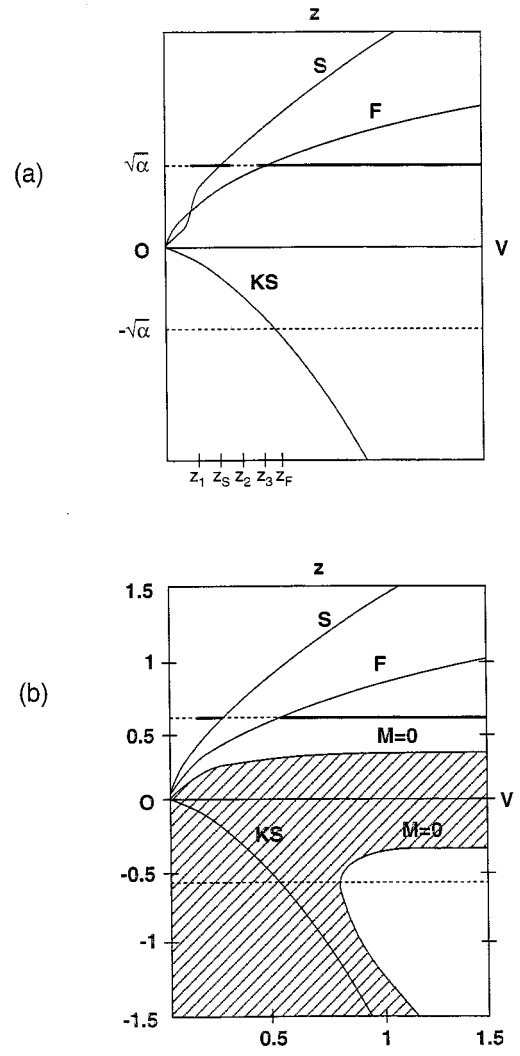

FIG. 1. This shows the form of $V(z)$ for the exact Friedmann (F), static (S) and Kantowski-Sachs (KS) solutions for (a) the general $\alpha<1/3$ case and (b) the $\alpha=1/3$ case. Also shown are the sonic lines $|V|=1/\sqrt{\alpha}$ (dotted) and the range of values of z (bold) in which one has a nodal sonic point ($z_1<z<z_2$ and $z>z_3$). Solutions described by one parameter (in particular, all subsonic ones) can only be regular if they cross the sonic line in this range. The condition $M=0$ corresponds to two curves in the $V(z)$ diagram for $\alpha=1/3$ and M is negative in the shaded region between these lines.

an analysis of their possible asymptotic behaviors and we now present this. For simplicity we will assume $z>0$ throughout this section but the analysis can be trivially extended to the $z<0$ case. We will also assume $\alpha>0$ except in the Kantowski-Sachs case. The full technicalities of the asymptotic analysis are presented elsewhere [20]. For present purposes it suffices to note that all self-similar solutions depend on powers of z at large and small values of $|z|$ or on powers of $\ln|z|$ at finite z. The last possibility arises because a finite value of z may sometimes correspond to zero or infinite physical distance. In this section we will identify these asymptotic states explicitly. We will show that there are three *exact* power-law solutions: the flat Friedmann solution, a Kantowski-Sachs solution and a static solution. We will also show that, for $\alpha>1/5$, there are solutions which asymptote to the Minkowski solution at either infinite or finite z. Finally there are solutions whose origin corresponds to a singularity at finite z. The validity of these results is confirmed by dynamical systems analyses [15,17,18]. In particular, the existence of the monotone and Dulac functions found in these analyses forbids the existence of periodic orbits and limit cycles and thereby excludes other possible asymptotic behaviors.

A. Power-law similarity solutions

In order to find the asymptotically ''power-law'' solutions explicitly, we look for solutions to the field equations of the form

$$x=x_o z^a, \quad S=S_o z^b \tag{3.1}$$

where x_o, S_o, a and b are constants. Note that $\dot{S}/S=b$ and $\dot{x}/x=a$. Equation (2.15) is satisfied if

$$a=\frac{b\alpha[3(b+1)+\alpha(3b+1)]}{(1+\alpha)[1+(1+\alpha)b]}. \tag{3.2}$$

The factor $[1+(1+\alpha)b]$ cannot be zero since this would be inconsistent with Eqs. (2.17) and (2.18). Equation (2.16) can then be written in the form

$$Az^p+Bz^q+C=0 \tag{3.3}$$

where

$$A\equiv\frac{b[(\alpha-1)+(1+\alpha)(2\alpha-1)b]}{\beta^2(1+\alpha)[1+(1+\alpha)b]}x_0^{2(1-\alpha)/\alpha}S_0^{-4},$$

$$B\equiv-(1+\alpha)x_0^{(1-\alpha)/\alpha}S_0^{-4},$$

$$C\equiv\frac{\alpha\gamma^2(b+1)[2+3b(1+\alpha)]}{(1+\alpha)[1+(1+\alpha)b]} \tag{3.4}$$

and the exponents are

$$p\equiv 2a\left(\frac{1-\alpha}{\alpha}\right)-4b+2\left(\frac{1-\alpha}{1+\alpha}\right), \quad q\equiv a\left(\frac{1-\alpha}{\alpha}\right)-4b. \tag{3.5}$$

Since B cannot be zero, there are three ways in which Eq. (3.3) can be satisfied to leading order as $z\to 0$ or $z\to\infty$ and we discuss these in turn. The first two cases correspond to solutions which satisfy the equations *exactly* but the third case only leads to asymptotic solutions.

$p=q$, $A+B=0$. In this case, the condition $p=q$ implies

$$a=-\frac{2\alpha}{1+\alpha} \tag{3.6}$$

and the condition $A+B=0$ implies

$$x_o^{(1-\alpha)/\alpha}=\frac{1}{2}\beta^2\left[\frac{(1+\alpha)^2}{b(1+\alpha)+1}\right]. \tag{3.7}$$

Equation (3.2) then requires

$$b=-1 \quad \text{or} \quad -\frac{2}{3(1+\alpha)} \tag{3.8}$$

and both values lead to $C=0$ from Eq. (3.4). Since Eq. (3.3) is satisfied exactly, there are no approximate solutions with $C\neq 0$.

The choice $b=-2/[3(1+\alpha)]$ corresponds to the flat Friedmann model. In this case, Eqs. (2.17) and (2.18) are satisfied if

$$x_o^{(\alpha-1)/\alpha}=\frac{2}{3\beta^2(1+\alpha)^2}, \quad \gamma^2 S_o^6 x_o^{-2/\alpha}=\frac{9(1+\alpha)^2}{(1+3\alpha)^2}, \tag{3.9}$$

and one can choose $x_o=S_o=1$ providing one scales the r and t coordinates such that

$$\beta=\frac{\sqrt{2}}{\sqrt{3}(1+\alpha)}, \quad \gamma=\frac{3(1+\alpha)}{(1+3\alpha)}. \tag{3.10}$$

This gives

$$x=z^{-2\alpha/(1+\alpha)}, \quad S=z^{-2/[3(1+\alpha)]} \tag{3.11}$$

and the metric becomes

$$ds^2=\beta^2\,dt^2-\gamma^{-2}z^{-4/[3(1+\alpha)]}\,dr^2 - r^{2(1+3\alpha)/[3(1+\alpha)]}\,t^{4/[3(1+\alpha)]}d\Omega^2. \tag{3.12}$$

One can put it in a more familiar form by making the coordinate transformation

$$\hat{t}=\beta t, \quad \hat{r}=\beta^{-2/[3(1+\alpha)]}r^{(1+3\alpha)/[3(1+\alpha)]}, \tag{3.13}$$

which gives

$$ds^2=d\hat{t}^2-\hat{t}^{4/[3(1+\alpha)]}[d\hat{r}^2+\hat{r}^2d\Omega^2]. \tag{3.14}$$

This is just the flat Friedmann solution with $p=\alpha\mu$. We also have

$$\mu=\frac{1}{4\pi t^2}, \quad V=\left(\frac{1+3\alpha}{\sqrt{6}}\right)z^{(1+3\alpha)/[3(1+\alpha)]}, \quad M=\tfrac{1}{3}z^{2(1+3\alpha)/[3(1+\alpha)]}. \tag{3.15}$$

The solutions asymptotic to this are discussed in Sec. IV B.

The choice $b=-1$ corresponds to the self-similar Kantowski-Sachs (KS) model. This is compatible with Eq. (3.7) providing

$$\beta^2=-\frac{2\alpha}{(1+\alpha)^2}x_o^{(1-\alpha)/\alpha}. \tag{3.16}$$

From Eqs. (2.17) and (2.18) we also require

$$S_o^2 x_o^{-(1+\alpha)/\alpha}=\frac{2\alpha}{(1+\alpha)^2-4\alpha^2}. \tag{3.17}$$

Equation (3.17) shows that we cannot take $x_o=S_o=1$ in this case but both x_o and S_o are determined in terms of α and β. The constant γ is not constrained at all. If we take β and γ to have the values given by Eq. (3.10) for $\alpha<0$ and i times those values for $\alpha>0$, so that we have the same r and t scaling as in the Friedmann solution, then Eqs. (3.16) and (3.17) give

$$x_0=\left(\frac{1}{3|\alpha|}\right)^{\alpha/(1-\alpha)}, \quad S_0^2=\frac{2\alpha}{(1+3\alpha)(1-\alpha)}\left(\frac{1}{3|\alpha|}\right)^{(1+\alpha)/(1-\alpha)}. \tag{3.18}$$

[Carr and Koutras [33] do not incorporate the i factors for $\alpha>0$ but this is a less sensible normalization since it allows the metric to be complex.] We now have

$$S=S_0 z^{-1}, \quad x=x_0 z^{-2\alpha/(1+\alpha)} \tag{3.19}$$

and the metric is

$$ds^2=\beta^2 x_0^2 dt^2-\gamma^{-2}x_0^{2/\alpha}S_0^{-4}z^{4\alpha/(1+\alpha)}dr^2-S_0^2t^2d\Omega^2. \tag{3.20}$$

The t coordinate is spacelike and the r coordinate is timelike for $\alpha>0$ because of the i factors in β and γ. For $-1/3<\alpha<0$, t and r have their usual interpretation but, from Eq. (3.18), the circumferential coordinate is timelike since S_o is imaginary. One can put the metric in a more familiar form by making the coordinate transformation

$$\hat{t}=\beta x_0 t, \quad \hat{r}=\gamma^{-1}(\beta x_0)^{2\alpha/(1+\alpha)}x_0^{1/\alpha}S_0^{-2}r^{(1+3\alpha)/(1+\alpha)}, \tag{3.21}$$

which gives

$$ds^2=d\hat{t}^2-\hat{t}^{-4\alpha/(1+\alpha)}d\hat{r}^2-(S_0/\beta x_0)^2\hat{t}^2d\Omega^2. \tag{3.22}$$

This corresponds to a KS solution with $p=\alpha\mu$. We also have

$$\mu t^2=\frac{1}{4\pi}\left(\frac{1}{3|\alpha|}\right)^{(1+\alpha)/(\alpha-1)}, \quad V=-\frac{(1-\alpha)(1+3\alpha)^2(3|\alpha|)^{2\alpha/(1-\alpha)}}{2\sqrt{6}\alpha}z^{(1+3\alpha)/(1+\alpha)}, \quad M=\frac{2\alpha^2}{(\alpha-1)(3\alpha+1)}\equiv M_{KS}. \tag{3.23}$$

V is negative for $0<\alpha<1$ (corresponding to tachyonic solutions), while M is negative for $-1/3<\alpha<1$ (corresponding to negative mass solutions). Presumably only solutions with

$\alpha<-1/3$ are physical. Note that Eq. (2.4) does not apply in this case because there is no well-defined origin; Eq. (3.19) implies that R is independent of r, so everything is on a shell. Instead the value of m must be interpreted as the mass of the whole Universe at time t, as indicated by Eq. (2.5). The solutions asymptotic to KS are discussed in Sec. IV C.

$q=0$, $B+C=0$. In this case, Eqs. (3.2) and (3.5) imply that the only consistent solution for $\alpha>0$ and $V>0$ is

$$a=b=0, \tag{3.24}$$

i.e. x and S are constant. [The condition $q=0$ permits another value of b but this leads to negative C for $\alpha>0$, so that the condition $B+C=0$ cannot be satisfied.] Equation (3.24) implies that A is zero and hence Eq. (3.3) is satisfied identically, so there are no approximate solutions with $A\neq 0$. The condition $B+C=0$ also requires

$$S_o^2=\frac{1+3\alpha}{\sqrt{18\alpha}}x_o^{(1-\alpha)/2\alpha} \tag{3.25}$$

for $\alpha>0$. This corresponds to the exact self-similar static solution, with the metric being given by

$$ds^2=\beta^2 x_o^2 z^{4\alpha/(1+\alpha)}dt^2-\gamma^{-2}x_o^{2/\alpha}S_o^{-4}dr^2-r^2S_o^2d\Omega^2. \tag{3.26}$$

This can be put in an explicitly static form

$$ds^2=\hat{r}^{4\alpha/(1+\alpha)}d\hat{t}^2-\gamma^{-2}x_o^{2/\alpha}S_o^{-6}d\hat{r}^2-\hat{r}^2d\Omega^2 \tag{3.27}$$

by introducing the variables

$$\hat{r}=rS_o, \quad \hat{t}=\left(\frac{1+\alpha}{1-\alpha}\right)\beta x_o S_o^{-2\alpha/(1+\alpha)}t^{(1-\alpha)/(1+\alpha)}. \tag{3.28}$$

The other relevant functions are

$$\mu=x_o^{-(1+\alpha)/\alpha}(4\pi r^2)^{-1}, \tag{3.29}$$

$$V=\sqrt{3\alpha}x_o^{(1-\alpha)/2\alpha}z^{(1-\alpha)/(1+\alpha)}, \quad M=\frac{2\alpha}{1+6\alpha+\alpha^2}.$$

If β and γ have the same values as in the Friedmann solution, corresponding to the same coordinate scaling, then Eqs. (2.17), (2.18) and (3.25) imply that x_o and S_o are given by

$$x_o=\left[\frac{(1+3\alpha)(1+6\alpha+\alpha^2)}{3(2\alpha)^{3/2}}\right]^{2\alpha/(1+3\alpha)}, \quad S_o=\left[\frac{(1+6\alpha+\alpha^2)^{(1-\alpha)/2}(\alpha+1/3)^{1+\alpha}}{2\alpha}\right]^{1/(1+3\alpha)}, \tag{3.30}$$

so there is only one static solution for each equation of state. This has been discussed by several authors [29,35,38]. Note that Eq. (2.20) implies that $V_R=0$ in this case, as expected. It should be stressed that there is no static solution in the *dust* case, essentially because one cannot put the $\dot{x}/\alpha$ term in Eq. (2.15) to zero. The solutions asymptotic to the static one are discussed in Sec. IV D.

Note that there is an interesting connection between the static and KS solutions: if one interchanges the r and t coordinates in metric (3.26) and also changes the equation of state parameter to

$$\alpha'=-\frac{\alpha}{1+2\alpha}, \tag{3.31}$$

one obtains the KS metric (3.20). For a static solution with a normal equation of state ($1>\alpha>0$), α' must lie in the range $-1/3$ to 0, so some negative pressure KS solutions are related to positive pressure static ones. However, the physical KS solutions with $-1<\alpha'<-1/3$ correspond to $|\alpha|>1$ and so do not give physical static solutions. Note that $\alpha=\alpha'$ only for $\alpha=0$ or $\alpha=-1$. The mass of both the static and KS solutions tends to 0 as $\alpha\to 0$, although the solutions do not exist in the limit $\alpha=0$ itself.

If one permits V to be negative, with β^2 and γ^2 reversing their sign, as in the KS solution, then the conditions $q=0$ and $B+C=0$ lead to another solution as $z\to\infty$ with

$$a=-\frac{4\alpha(\alpha^2+6\alpha+1)}{(7\alpha+1)(1-\alpha^2)}, \quad b=-\frac{(\alpha^2+6\alpha+1)}{(7\alpha+1)(1+\alpha)} \tag{3.32}$$

providing

$$S_o^2=x_o^{(1-\alpha)/2\alpha}\sqrt{\frac{(7\alpha+1)(1-\alpha)}{18\alpha}}. \tag{3.33}$$

This implies that $S\to 0$ and $\mu r^2\to\infty$. One also has

$$V\sim z^{-(3\alpha+1)^2/[(7\alpha+1)(1+\alpha)]}, \qquad M\sim z^{2(3\alpha+1)(\alpha^2+6\alpha+1)/[(7\alpha+1)(1-\alpha^2)]}, \tag{3.34}$$

so $V\to 0$ and $M\to\infty$. This limiting behavior arises in the discussion of Sec. IV C.

$p=0$, $A+C=0$. The condition $p=0$ implies

$$b=\frac{1}{2}\left(\frac{1-\alpha}{\alpha}\right)a+\frac{1}{2}\left(\frac{1-\alpha}{1+\alpha}\right) \tag{3.35}$$

and Eq. (2.19) then requires that V tend to the finite value

$$V_*=\beta^{-1}\gamma^{-1}x_o^{(1-\alpha)/\alpha}S_0^{-2}. \tag{3.36}$$

The condition $A+C=0$ now implies

$$a=\frac{V_*^2(1-\alpha)+2\alpha}{(V_*^2-1)(1+\alpha)},\quad b=\frac{(1-\alpha)(V_*^2+\alpha)}{2\alpha(1+\alpha)(V_*^2-1)}, \tag{3.37}$$

while Eq. (3.5) yields

$$q=\frac{(1-\alpha)V_*^2}{\alpha(1-V_*^2)}. \tag{3.38}$$

It should be emphasized that, since $B\neq 0$ from Eq. (3.4), this does not lead to an *exact* solution.

Equation (3.38) is only a consistent solution of Eq. (3.3) for large z if $V_*^2>1$ and for small z if $V_*^2<1$. In the latter case, Eq. (3.37) implies that both a and b are negative, so the density goes to infinity and the scale factor goes to zero. However, Eq. (2.17) gives negative values of M (and hence unphysical solutions) unless $V_*^2<\alpha$ and this last condition will also turn out to be inconsistent. We therefore focus on the $V_*^2>1$ case. Equation (3.34) then implies that both a and b are positive, so the density goes to zero and the scale factor goes to infinity. Equation (2.17) gives

$$M\sim\left(\frac{V^2-\alpha}{V^2-1}\right)z^{-[V_*^2(1-\alpha)+1+3\alpha]/(V_*^2-1)(1+\alpha)} \tag{3.39}$$

and this necessarily tends to zero as $z\to\infty$. [The coefficient has been included to demonstrate that the mass is negative for $1>V_*^2>\alpha$.] On the other hand, Eq. (2.18) implies

$$M-\frac{1}{2}\sim z^{[V_*^2(1-\alpha)-\alpha(1+3\alpha)]/(V_*^2-1)\alpha(1+\alpha)}\times[b^2(V_*^2-1)-2b-1]. \tag{3.40}$$

If the exponent of z in this expression is positive, $M\to 0$ as $z\to\infty$ only if the term in square brackets does and this requires $b=1/(V_*-1)$. Equation (3.37) then gives a quadratic equation for V_*:

$$(1-\alpha)V_*^2-2\alpha(1+\alpha)V_*-\alpha(1+3\alpha)=0 \tag{3.41}$$

with the real positive solution

$$V_*=\frac{\alpha(1+\alpha)+\sqrt{\alpha(\alpha^3-\alpha^2+3\alpha+1)}}{1-\alpha}. \tag{3.42}$$

Note that Eq. (3.41) implies that the exponent of z in Eq. (3.40) is indeed positive (as assumed). Also V_* decreases from ∞ to $\sqrt{\alpha}$ as α decreases from 1 to 0, which precludes $V_*<\sqrt{\alpha}$, so there are no subsonic solutions of this kind as $z\to 0$. The value of V_* given by Eq. (3.42) exceeds 1 (as required) only for $\alpha>1/5$, so these solutions do not exist in the dust case. In the special case $\alpha=1/3$, $V_*=(2+\sqrt{13})/3=1.9$.

Equations (3.36) and (3.42) impose a relationship between x_0 and S_0, so these solutions are described by just one independent parameter. Requiring that the right-hand side of Eq. (3.40) tends to $-1/2$ as $z\to\infty$ merely determines the second order terms in the expansions for x and S. The metric has the asymptotic form

$$ds^2\sim z^{2V_*^2/(V_*^2-1)}dt^2-z^{2/(V_*^2-1)}dr^2-r^2z^{2/(V_*-1)}d\Omega^2 \tag{3.43}$$

and this can be reduced to the Minkowski form with a suitable change of coordinates [10]. The leading terms in the components of the Ricci tensor are given by

$$R_t^t\sim R_r^r\sim R_\theta^\theta\sim R_\phi^\phi\sim r^{-2V_*^2/(V_*^2-1)}. \tag{3.44}$$

These always decrease at least as fast as r^{-2} as $r\to\infty$ and the fall-off becomes arbitrarily fast as $\alpha\to 1/5$. Although $MS\to 0$ as $z\to\infty$, it does so slower than z^{-1}, so that the mass itself ($m=rMS$) diverges. Since Eq. (3.42) implies $V_*\to\infty$ in the limit $\alpha\to 1$, Eq. (3.43) then reduces to the static metric [cf. Eq. (3.26)]. One can also see this from Eq. (3.37), which implies $a=b=0$ in this limit, so the scale factor no longer diverges and the density no longer goes to zero.

The forms of $V(z)$ for the Friedmann, static and KS solutions are shown in Fig. 1(a) for the general $\alpha<1/3$ case and in Fig. 1(b) for the $\alpha=1/3$ case. Note that the exponent of z is smaller for the Friedmann solution than the static solution if $\alpha<1/3$, so the Friedmann velocity is smaller as $z\to\infty$ but larger as $z\to 0$. For $\alpha>1/3$, the situation is reversed. The exponents are the same for $\alpha=1/3$ and the Friedmann velocity is always smaller. The asymptotically Minkowski solutions for $\alpha>1/5$ are not included since they are not *exact* (viz. Minkowski has no matter). Note also that the Minkowski solution, although static, is distinct from the exact self-similar static solution given by Eq. (3.26).

A rather peculiar feature of the similarity solutions, which arose in the context of the KS model, is that the mass can go negative. This may seem unphysical but—in the context of the big bang model—Miller [39] has given a possible interpretation of this in terms of ''lagging'' cores. In the $\alpha=1/3$ case (and *only* this case), Carr and Koutras [33] show that there is a curve in the $V(z)$ diagrams where $M=0$:

$$V^3=-\sqrt{3/2}\;z^{3/2}(V^2-1/9) \tag{3.45}$$

and this is also shown in Fig. 1(b). One sees that the curve has asymptotes at $V=\pm 1/3$. The upper part (with $V>1/3$) is relevant for asymptotically Friedmann solutions, while the lower part (with $V<-1/3$) is relevant for asymptotically KS solutions. M is negative in between the two parts and this region includes KS itself (as expected). Note that Eq. (3.45) is not a *sufficient* condition for $M=0$; it implies that M has two possible values, only one of which is zero.

B. Logarithmic power-law similarity solutions

By analogy with Eq. (3.1) we now look for solutions in which z tends to some finite value z_* and in which

$$x=x_0|L|^a,\quad S=S_0|L|^b,\quad L\equiv\ln(z/z_*) \tag{3.46}$$

for constants x_0 and S_0. (The modulus signs are required since L may be negative and may appear with fractional exponents.) Clearly $z=z_*$ corresponds to an infinite distance from the origin for $b<0$ and zero distance for $b>0$. Equation (2.15) requires

$$b\left[3b-1-\left(\frac{1+\alpha}{\alpha}\right)a\right]+\left[\left(\frac{3+\alpha}{1+\alpha}\right)b-\frac{a}{\alpha}\right]L=0 \quad (3.47)$$

and the leading term is zero only for

$$b=\frac{1}{3}+\left(\frac{1+\alpha}{3\alpha}\right)a. \quad (3.48)$$

It turns out that the last term in Eq. (3.47) is never zero, so these are only asymptotic and not exact solutions. There are now two possible situations, according to whether V tends to infinity or some constant value V_*.

$V\to V_*$ as $z\to z_*$. In this case, Eq. (2.16) can be written in the form

$$aL^{-1}=\frac{2V^2\alpha b}{(V^2-\alpha)}L^{-1}+\frac{2\alpha^2}{(1+\alpha)(V_*^2-\alpha)} -\frac{\alpha(1+\alpha)\beta^2V_*^2}{V_*^2-\alpha}z_*^{-2(1-\alpha)/(1+\alpha)}(x_0|L|^a)^{(\alpha-1)/\alpha} \quad (3.49)$$

where the first term contains V rather than V_* because the factor $(V^2-V_*^2)L^{-1}$ may go to a constant as $z\to z_*$. The only consistent solution to this equation has the last term tending to zero (i.e. $a<0$) and this then implies

$$a=\left(\frac{2V_*^2\alpha}{V_*^2-\alpha}\right)b. \quad (3.50)$$

However, Eq (2.19) also implies

$$a=\left(\frac{2\alpha}{1-\alpha}\right)b, \quad (3.51)$$

so we require $V_*^2=1$. Equations (3.48) and (3.51) determine a and b and lead to

$$S\approx S_0|L|^{(1-\alpha)/(1-5\alpha)}, \quad x\approx x_0|L|^{2\alpha/(1-5\alpha)}. \quad (3.52)$$

Thus the scale factor diverges and the density goes to zero providing $\alpha>1/5$. [The scale factor goes to zero and the density diverges for $\alpha<1/5$ but these solutions would have negative mass (see below), so we neglect them.] The condition $V_*=1$ gives a relationship between the constants x_0, S_0 and z_* from Eq. (2.19), so these solutions are described by two independent parameters.

Equation (2.17) now implies

$$M\sim\left(\frac{1-\alpha}{5\alpha-1}\right)|L|^{(1-\alpha)/(5\alpha-1)}, \quad (3.53)$$

so this is zero at $z=z_*$. [The coefficient demonstrates that the mass would be negative for $\alpha<1/5$.] One also requires z to tend to z_* from *below* else M would be negative. Equation (2.18) can be written as

$$M=\frac{1}{2}+\frac{1}{2}\gamma^2x^{-2/\alpha}S^6\left\{\left(\frac{\dot S}{S}\right)^2(V^2-1)-\frac{2\dot S}{S}-1\right\}. \quad (3.54)$$

Since $x^{-2/\alpha}S^6\sim|L|^{2(3\alpha-1)/(5\alpha-1)}$ goes to infinity for $\alpha<1/3$ and zero for $\alpha>1/3$, one requires the term in curly brackets in Eq. (3.54) to go to zero and infinity, respectively, in these two cases. However, the last term in Eq. (3.54) can also be written as

$$\sim|L|^{(\alpha-1)/(5\alpha-1)}\left[\frac{\dot S}{S}(V^2-1)-2-\frac{S}{\dot S}\right]. \quad (3.55)$$

Since the exponent of $|L|$ is negative, we need the term in square brackets to go to zero for all α and to scale as $|L|^{(1-\alpha)/(5\alpha-1)}$. Therefore one always requires

$$\frac{\dot S}{S}(V^2-1)\to 2 \quad (3.56)$$

and Eqs. (2.19) and (3.49) then imply

$$\frac{\dot V}{V}\to\frac{1-5\alpha}{1-\alpha}<0, \quad (3.57)$$

where we have used the approximation

$$\frac{V^2}{V^2-\alpha}\approx\frac{1}{1-\alpha}\left[1-\left(\frac{\alpha}{1-\alpha}\right)(V^2-1)\right]. \quad (3.58)$$

However, the way in which condition (3.56) is satisfied depends on the value of α and requires a higher order analysis. In general, we can write

$$S\approx S_0|L|^b(1+A|L|^k+CL), \quad x\approx x_0|L|^a(1+B|L|^k+DL) \quad (3.59)$$

where a and b are given by Eq. (3.52) and (k,A,B,C,D) are constants to be determined. Equations (3.53) and (3.54) impose a relationship of the form

$$O(|L|^{(1-\alpha)/(5\alpha-1)})=1+O(|L|^{(\alpha-1)/(5\alpha-1)}) \times\left[\frac{\dot S}{S}(V^2-1)-2-\frac{S}{\dot S}\right] \quad (3.60)$$

and matching the exponents of $|L|$ implies $k=(1-\alpha)/(5\alpha-1)$. For $\alpha>1/3$, one has $k<1$ and so the leading term in Eq. (3.59) goes like L^k. For $\alpha<1/3$, one has $k>1$, so it goes like L. In both cases, inserting the expressions for S and x given by Eq. (3.59) into Eq. (3.60) uniquely determines the constants (A,B,C,D) but does not impose any further relationship between x_0, S_0 and z_*.

In order to understand the physical significance of these solutions, we note that the metric can be written as

$$ds^2 \sim |L|^{4\alpha/(1-5\alpha)}[dt^2 - dr^2 - r^2|L|^{2(3\alpha-1)/(5\alpha-1)}d\Omega^2]. \tag{3.61}$$

A calculation of the Ricci tensor then shows that the leading terms are given by

$$R_t^t \sim R_r^r \sim R_\theta^\theta \sim R_\phi^\phi \sim r^{-2}(z-z_*)^{-(1-\alpha)/(5\alpha-1)}. \tag{3.62}$$

For $1/5<\alpha<1$, the curvature goes to zero as $z \to z_*$, so these solutions are flat along the limiting similarity hypersurface; this hypersurface is null since $V_*=1$. Although r tends to a finite value for finite t, this is just a coordinate anomaly since Eq. (3.52) implies that the physical distance diverges. For $\alpha=1/3$, Eq. (3.61) implies that the metric is conformally flat. In this case, one can understand these features as arising because the metric resembles the open Friedmann model, so that it can be transformed to Minkowski form as $z \to z_*$ with a new choice of time-slicing (as in the Milne model). These solutions can therefore be regarded as asymptotically Minkowski or, more precisely, asymptotically Schwarzschild since Eqs. (3.52) and (3.53) imply that $m=MSr$ tends to a constant. They are discussed further elsewhere [10]. Note that Eq. (3.52) shows that the scale factor no longer diverges at z_* in the limit $\alpha=1$, although the density still goes to zero.

$V \to \infty$ as $z \to z_*$. In this case, Eq. (2.16) can be written in the form

$$aL^{-1} = 2\alpha b L^{-1} - \alpha(1+\alpha)\beta^2 z_*^{-2(1-\alpha)/(1+\alpha)} \times (x_0|L|^a)^{(\alpha-1)/\alpha}. \tag{3.63}$$

It is easy to show that the only consistent solution has $a=\alpha/(1-\alpha)$, so that all the terms scale as L^{-1}, and Eq. (3.48) then implies $b=2/[3(1-\alpha)]$. Since

$$S \approx S_0|L|^{2/3(1-\alpha)}, \quad x \approx x_0|L|^{\alpha/(1-\alpha)}, \tag{3.64}$$

the scale factor goes to zero and the density goes to infinity at z_*, so this corresponds to a singularity at the physical origin. Equation (2.17) also gives

$$M \sim |L|^{-2/3(1-\alpha)}, \tag{3.65}$$

so $M \to \infty$ and MS tends to a constant at $z=z_*$. In order for the mass to be positive, z must also approach z_* from *above*. Note that Eq. (3.63) yields the same relation between A, B and z_* as Eqs. (2.17) and (2.18), so these solutions are described by two independent parameters. Equations (2.13) and (2.14) imply that the metric tends to

$$ds^2 \sim |L|^{2\alpha/(1-\alpha)}dt^2 - |L|^{-2/3(1-\alpha)}dr^2 - r^2 L^{4/3(1-\alpha)}d\Omega^2, \tag{3.66}$$

corresponding to a Schwarzschild-type singularity in that $g_{tt} \to 0$ and $g_{rr} \to \infty$.

IV. SELF-SIMILAR SOLUTIONS WITH PRESSURE

Having derived the possible asymptotic behaviors of self-similar solutions at large and small distances, we can now obtain the complete family of solutions by taking all possible combinations. Apart from the asymptotically Kantowski-Sachs solutions, which are confined to $V<0$ for $0<\alpha<1$ and therefore form a disjoint family, there are three possible behaviors at large distances (associated with the Friedmann, static and Minkowski solutions) and three possible behaviors at small distances (associated with the Friedmann, static and centrally singular solutions). One might therefore expect there to be nine types of solutions in $V>0$. However, six of these would involve a sonic point, so one needs to check which of them could be regular there. In this section we will first sketch the overall qualitative features of the solutions and then consider some of them in more detail. We will need to consider both signs of z since some families necessarily span both signs.

A. General characteristics of solutions

An important step in classifying the full family of self-similar solutions with pressure is a determination of the number of free parameters associated with each of the asymptotic behaviors. Once this is known, one can deduce many of the qualitative features of the classification by simple parameter-counting, so one of the purposes of the discussion later in this section is to determine this. We will anticipate the results of that discussion in our initial qualitative considerations. The supersonic and subsonic regimes, which usually correspond to large and small values of $|z|$ respectively, will be considered separately because they have very different characteristics. We will then discuss the asymptotically singular regime.

Supersonic solutions

In the supersonic regime one might expect the $\alpha>0$ solutions to share some of the qualitative features of the $\alpha=0$ ones. The arguments for this are partly physical (viz. pressure effects should be unimportant on sufficiently large scales) and partly mathematical (viz. the dust equations can be obtained from the general α equations by taking the limit $\alpha \to 0$). We will therefore start by recalling the behavior of the dust solutions [13].

As in the general α case, the most general dust solution is described by two parameters. The first one (E) corresponds to the energy, this being conserved (i.e. independent of z) if $\alpha=0$; the second one (D) specifies the value of z at the singularity which characterizes such models. The 1-parameter family of solutions with $z>0$ and $D=0$ are inhomogeneous cosmological models which expand from a big bang singularity at $z=\infty$ and are asymptotically Friedmann at large z; models with $E>0$ are underdense and expand faster than Friedmann, while those with $E<0$ recollapse to black holes and contain another singularity. The $D=0$ solutions with $z<0$ are just the time reverse of the $z>0$ ones. The 2-parameter solutions with $D>0$ again represent inhomogeneous models but they involve both $z<0$ and $z>0$ regimes and, while there is no exact static solution in the dust

case, they are asymptotically ''quasi-static'' (in a sense to be defined later) at large $|z|$. The solutions with $E \geqslant 0$ either expand monotonically from a big bang singularity at $z = -1/D$ or contract monotonically to a big crunch singularity at $z = +1/D$, whereas the ones with $E<0$ recollapse to or expand from a second singularity. The $D<0$ solutions contain a shell-crossing singularity and are probably unphysical.

The behavior of the dust solutions suggests that there should exist at least two classes of self-similar solutions with pressure at large $|z|$: a 1-parameter family which are asymptotically Friedmann and a 2-parameter family which are asymptotically quasi-static. We will show that there are indeed solutions of these kinds. However, we saw in Sec. III that new possible behaviors arise at large $|z|$ when there is pressure. In particular, there is an exact static solution and an exact KS solution, so one might expect there to be families of solutions asymptotic to these. We will confirm that this is the case and demonstrate that each of the families is described by one parameter at large $|z|$. We also saw in Sec. III that there is a 1-parameter and a 2-parameter family of asymptotically Minkowski solutions for $\alpha > 1/5$.

Subsonic solutions

The inclusion of pressure obviously introduces qualitatively new features in the subsonic regime, so there are important differences from the dust solutions at small values of $|z|$. In particular, we have seen that the presence of a sonic point at $|V| = \sqrt{\alpha}$ allows solutions to be discontinous there, so one might anticipate a wide variety of transonic behaviors. However, the requirement that the solution be *regular* at the sonic point (i.e. intersecting the sonic surface on the line Q discussed in Sec. II, so that it has finite pressure gradient and no shock) severely restricts the behavior there. Furthermore, all *physical* subsonic solutions must reach $z=0$ and this will only be true for some subset of the regular ones. We will show that the only possible solutions at small $|z|$ are the exact static model, a 1-parameter family of asymptotically Friedmann (or ''regular center'') models and a 1-parameter family of asymptotically KS models. In order to determine which combination of supersonic and subsonic solutions are possible, we will use simple parameter-counting arguments.

We saw in Sec. II that from each *saddle* sonic point ($z < z_1$) there emanates just one transonic solution and parameter-counting indicates that this is likely to be a member of a family described by two parameters asymptotically. This means that such a solution is unlikely to reach $z=0$ (since solutions are described by at most one parameter there) and so unlikely to be physical in the subsonic regime. However, for any particular value of α, parameter-counting indicates that one could still expect a discrete subset of saddle point subsonic solutions to be physical; these would need to be analytic at the sonic point and probably members of a 2-parameter family in the supersonic regime (i.e. asymptotically quasi-static or Minkowski at large $|z|$). For some range of α, this includes the solution which arises in the context of critical phenomena [10].

From each *nodal* sonic point ($z_1 < z < z_2$, $z > z_3$) we saw that there emanate both an isolated ''secondary'' solution and a 1-parameter family of ''primary'' solutions. The same considerations apply for the isolated solution as for the saddle point solution but parameter-counting indicates that the primary solutions could also contain a member of a family described by one parameter asymptotically. Thus in this situation there *could* be a physical solution in the subsonic regime from each sonic point and this might also connect to a supersonic solution which is asymptotically Friedmann, static or Minkowski as $|z| \to \infty$. However, one finds that such solutions only exist for bands of values for the asymptotic parameters, each band being characterized by the number of oscillations in the fluid velocity in the subsonic regime [19]. Since the static solution always has a nodal sonic point, for each value of α one could also expect just one member of each 1-parameter family of supersonic solutions and a 1-parameter subset of each 2-parameter family of such solutions to match onto the static subsonic solution.

The nodal solutions would generally be C^1 at the sonic point. However, the isolated secondary solution and one member of each band of primary solutions would also be analytic or at least C^∞. Such solutions would generally have to connect to a member of a 2-parameter family in the supersonic regime and would not reach the origin. However, as in the case of a saddle point, one could still expect a discrete subset of them to connect to a member of a 1-parameter family for a given value of α. The only analytic solutions in the first band are the Friedmann model (this being primary for $\alpha < 1/3$ or secondary for $\alpha > 1/3$) and the general relativistic version of the Larson-Penston solution [7,19] for sufficiently low α (this always being secondary). In the KS case with $\alpha > 0$ there are only isolated solutions at the sonic point; since asymptotically KS solutions are described by one parameter at both large and small $|z|$, none of those hitting the sonic surface are likely to be regular there.

These considerations make it clear that most regular solutions emanating from a sonic point will not be physical in the subsonic regime: this is just a consequence of the fact that the solutions passing through $z=0$ are described by one less parameter than those emanating from the line Q. Most subsonic solutions will either enter a negative mass regime [i.e. in the $\alpha = 1/3$ case they will cross the line given by Eq. (3.45)] or they will hit the sonic surface again but off the line Q. For the same reason, not all the solutions from $z=0$ will reach the sonic surface on the line Q and even those that do may not do so at a node. In this paper we will only focus on the physical solutions but it should be appreciated that the full solution space contains many other non-physical ones.

Singular solutions

Many of the self-similar solutions exhibit a central curvature singularity and this will then correspond to the physical origin (even though the value of z may be non-zero). Some of the solutions contain *two* singularities (with different signs of z), one giving the origin for $t<0$ and the other for $t>0$. As in the dust case, these singularities are generally characterized by the fact that the velocity function $V(z)$ goes infinite and, since V tends either to infinity as $|z| \to \infty$ or to a

supersonic value V_* as $|z|\to z_*$, this suggests that solutions containing them are likely to be supersonic *everywhere*. For if such a solution had a subsonic regime, it would need to cross the sonic surface *twice*, including once at a saddle point (where $\dot{V}$ may be negative and there are only isolated solutions), so parameter-counting makes it unlikely that such a solution could exist. The form of the dust solutions suggests that the asymptotically singular solutions should be described by two parameters, one being the value of z at the singularity itself (z_S), and this was confirmed by the analysis in Sec. III. For each value of z_S, one could therefore expect at most one of the solutions to be a member of a family described by one parameter at large distance; the rest would have to be members of a family described by two parameters. An interesting feature of the singular self-similar solutions is that the singularity can be naked [19]. Note that there are also solutions with ''mild'' singularities, in which V does not diverge. For example, the static solution contains a (naked) central singularity at $z=0$, even though $V=0$ there.

The important conclusion of these qualitative considerations is that the large-distance behavior of solutions ''almost'' uniquely specifies their small-distance behavior. This is necessarily the case for solutions which contain no sonic point and, even if there is a sonic point, one can only extend a supersonic solution into the subsonic regime in a small number of ways (if at all). It is therefore convenient to *classify* the solutions according to their behavior at large distances alone. This gives four classes of solution and in the rest of this section we will consider these in turn. We will start by discussing the characteristics of the asymptotically Friedmann and asymptotically KS solutions. In this context we will be mainly reviewing the work of Carr and Yahil [29] and Carr and Koutras [33] but we will extend these earlier studies somewhat, explain some of their features in terms of the results obtained in Sec. III and make the connection with the dust solutions more explicit. We will then discuss the asymptotically quasi-static solutions. The discussion here will be mainly original, although some examples of this type of solution have been considered before [19,36]. The asymptotically Minkowski solutions are entirely new but will only be discussed briefly; they are treated in more detail elsewhere [10]. In each case we will present the form of the functions $S(z)$ and $V(z)$ since these have an obvious physical significance. The form of the function $V(z)$ for all these solutions is brought together in Fig. 6 for the $\alpha=1/3$ case.

B. Asymptotically Friedmann solutions

Carr and Yahil [29] consider solutions which are either exactly or asymptotically Friedmann for large and small values of z. They therefore introduce functions $A(z)$ and $B(z)$ defined by

$$x\equiv z^{-2\alpha/(1+\alpha)}e^{A}, \quad S\equiv z^{-2/3(1+\alpha)}e^{B}. \tag{4.1}$$

(They assume $z>0$, as we do here; otherwise z must be replaced by $|z|$ in what follows.) The Friedmann solution itself ($A=B=0$) passes through the sonic line Q at

$$z_F=\left[\frac{\sqrt{6\alpha}}{1+3\alpha}\right]^{3(1+\alpha)/(1+3\alpha)}. \tag{4.2}$$

For comparison the static solution passes through Q at

$$z_S=\left[\frac{(2\alpha)^{3/2}3^{(5\alpha-1)/2(\alpha-1)}}{(1+3\alpha)(1+6\alpha+\alpha^2)}\right]^{(1+\alpha)/(1+3\alpha)} \tag{4.3}$$

and one can show that this is always less than z_F. In fact, the only physical subsonic solution which passes through z_F is the Friedmann solution itself. All the other solutions are unphysical because, as z decreases, V either reaches a minimum and then hits the sonic surface again but off the line Q or the mass within r goes negative. This was first demonstrated by Bicknell and Henriksen [26] but it is also a consequence of the general considerations given in Sec. IV A. For since there should only be one physical subsonic solution from each nodal point, this must be the Friedmann solution itself if the point is z_F. Since the only physical solution which is exactly Friedmann outside the sonic point is the Friedmann solution *everywhere*, we henceforth confine attention to solutions which are asymptotically Friedmann.

We first consider the solutions which are asymptotically Friedmann as $z\to\infty$ (i.e. as $r\to\infty$ for fixed t or as $t\to 0$ for fixed r). The ordinary differential equations for x and S become ordinary differential equations for A and B. If we linearize these equations in A, $\dot{A}$ and $\dot{B}$ to find the 1st order solution as $z\to\infty$, Eqs. (2.15) and (2.16) yield

$$\ddot{B}=\left(\frac{1}{3\alpha}\right)\dot{A}-\left(\frac{1+3\alpha}{1+\alpha}\right)\dot{B}, \tag{4.4}$$

$$\dot{B}=\left(\frac{1}{2\alpha}\right)\dot{A}-\frac{(\alpha-1)}{3\alpha(1+\alpha)}A. \tag{4.5}$$

Differentiating the second equation and eliminating $\dot{B}$ and $\ddot{B}$ then leads to the following differential equation for A:

$$\ddot{A}+\frac{(9\alpha-1)}{3(1+\alpha)}\dot{A}+\frac{2(1+3\alpha)(\alpha-1)}{3(1+\alpha)^2}A=0. \tag{4.6}$$

This has two solutions,

$$A\sim z^{-2(1+3\alpha)/3(1+\alpha)} \quad \text{or} \quad A\sim z^{(1-\alpha)/(1+\alpha)}, \tag{4.7}$$

but the second one can be rejected since the exponent is positive for $\alpha<1$ (so that A diverges as $z\to\infty$). The first solution gives

$$\begin{aligned} A&=-\frac{\alpha(1+3\alpha)}{(1+\alpha)}kz^{-2(1+3\alpha)/3(1+\alpha)},\\ B&=B_\infty-kz^{-2(1+3\alpha)/3(1+\alpha)} \end{aligned} \tag{4.8}$$

where $B_\infty\equiv B(\infty)$ and k are integration constants. Note that $A\to 0$ as $z\to\infty$ because Eqs. (2.12) and (4.1) show that the asymptotic value of A has physical significance (viz., the asymptotic density perturbation) but there is no physical re-

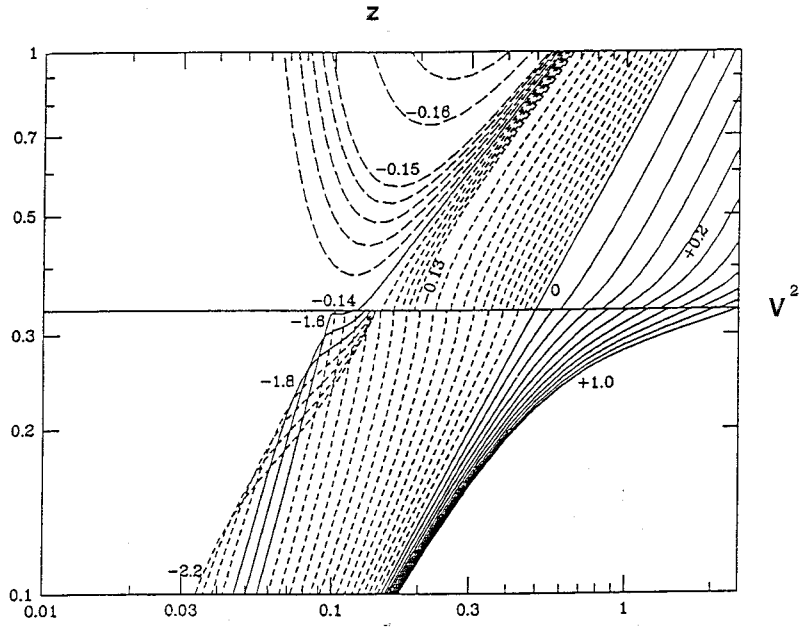

FIG. 2. This shows the form of the function $V(z)^2$ for the asymptotically Friedmann solutions with a radiation equation of state ($\alpha = 1/3$), with particular emphasis on the behavior at the sonic point. Solutions which are regular (irregular) at the sonic point are shown by solid (short-broken) lines, while black hole solutions (with no sonic point) are shown by long-broken lines. Only the first band of overdense solutions are shown. The curves are labeled by B_∞ in the supersonic regime (with a spacing of 0.01 or 0.05) and by A_0 in the subsonic regime (with a spacing of 0.1). There is a 1-parameter continuum of regular underdense solutions but the overdense solutions lie in discrete bands and are characterized by the number of oscillations they exhibit; just one solution in the first band is shown.

striction on B_∞ (the asymptotic value of B). The constants in Eq. (4.8) are related since Eqs. (2.17) and (2.18) imply

$$k = \frac{3(1+\alpha)(e^{-2B_\infty} - e^{4B_\infty})}{2(1+3\alpha)(5+3\alpha)}. \tag{4.9}$$

Thus there is a 1-parameter family of asymptotically Friedmann solutions. [Despite the presence of the parameter B_∞, these solutions are really asymptotic to the *exact* Friedmann model, since one could formally gauge B_∞ to zero at infinite (but not finite) z by taking a different spatial hypersurface.] From Eq. (2.21), the energy function is

$$\mathcal{E} = E + O(z^{-4(1+3\alpha)/3(1+\alpha)}), \quad E = \frac{1}{2}(e^{6B_\infty} - 1) \tag{4.10}$$

where the asymptotic energy E is equivalent to the parameter E which arose in the dust case. Equation (2.12) shows that the solutions are overdense or underdense relative to the Friedmann solution according to whether $A<0$ or $A>0$, respectively. From Eqs. (4.9) and (4.10), this corresponds to $(k>0, B_\infty<0, E<0)$ or $(k<0, B_\infty>0, E>0)$, respectively. In the Friedmann case itself, $k = B_\infty = E = 0$.

The form of $V(z)$ in these solutions is shown in the upper part of Fig. 2, where the curves are labeled by the value of B_∞. The figure assumes $\alpha = 1/3$ but retains the same qualitative features for other values of α. If B_∞ is sufficiently negative, V reaches a minimum value $V_{\min}$ above $\sqrt{\alpha}$ as z decreases and then rises again to infinity at the singularity ($z = z_S$). The form of the solution near z_S is given by Eq. (3.64). There is a 1-parameter family of solutions for a given value of z_S but presumably only one of these could be asymptotically Friedmann. Such solutions are supersonic everywhere and contain black holes which grow as fast as the Universe. There is an event horizon and particle horizon providing $V_{\min}<1$ and this will apply if B_∞ is more than some critical negative value B_∞^*; otherwise the whole Universe is inside the black hole. However, since Eqs. (2.15) and (2.17) imply that $\dot{M} = 0$ at $\dot{S} = 0$ and Eq. (2.18) then implies $M < 1/2$, we infer that M always has a minimum below 1/2. Thus there is always an *apparent* horizon; this generalizes the result found in the dust case. For this reason, it is convenient to regard the apparent horizon rather than the event horizon as defining the boundary of the black hole. The mass of the hole can then be taken to be $m_{BH} = (MSz)_{BH}t$, whereas the mass of the singularity is $m_S = (MSz)_S t$. Both masses are initially zero and then grow as t.

As B_∞ increases (i.e. as the asymptotic overdensity decreases), the values of $V_{\min}$ and $z_{\min}$ decrease. Eventually it reaches another critical negative value B_∞^{crit} at which $V_{min} = \sqrt{\alpha}$ and, for $B_\infty > B_\infty^{crit}$, the solutions must reach the sonic surface. As B_∞ continues to increase, the value of z at which the solution goes transonic (z_s) increases, passing through the value indicated by Eq. (4.2) when $B_\infty = 0$ and tending to infinity as B_∞ goes to infinity (corresponding to increasingly underdense solutions). All the solutions with $B_\infty > B_\infty^{crit}$ reach the sonic surface but only the ones which cut it on the line Q are regular. This applies if z_s lies within the ranges z_1 to z_2

or above z_3 [indicated in Fig. 1]. $\dot{A}$ diverges at the sonic point for values of B_∞ corresponding to $z_2<z_s<z_3$.

We next consider the condition that the solution be asymptotically Friedmann as $z\to 0$ (i.e. as $t\to\infty$ for fixed r or as $r\to 0$ for fixed t). Goliath et al. [17] describe these solutions as having a ''regular center.'' Since we require $S\to\infty$ and $V\to 0$ in the limit $t\to\infty$, we need A and B to be finite, which implies

$$\dot{A}(0)=\dot{B}(0)=0. \tag{4.11}$$

Also $m/r=MS$ must be finite in the limit $r\to 0$, so we require $M(0)=0$. (This condition distinguishes these solutions from the static one, which has $m/r\to\infty$ as $r\to 0$.) Equation (2.18) then implies

$$A(0)=3\alpha B(0), \tag{4.12}$$

which shows that there is a 1-parameter family of solutions which are asymptotically Friedmann at $z=0$. We will take this parameter to be $A_0\equiv A(0)$. This is a measure of the overdensity (either at the origin for fixed t or at late times for fixed r) since, from Eqs. (2.12) and (4.1),

$$A_0=\left[\frac{\alpha}{1+\alpha}\right]\log\left[\frac{\mu_F(0)}{\mu(0)}\right] \tag{4.13}$$

where μ_F is the density in the Friedmann solution. Thus $A_0>0$ and $A_0<0$ solutions are underdense and overdense, respectively. In contrast to the dust case, where the density goes to zero at $z=0$ for the $(E>0)$ asymptotically Friedmann solutions, one always has a uniform density core for small z. Note that Eqs. (2.21) and (4.12) imply that $\mathcal{E}\to 0$ as $z\to 0$.

For some range of values of A_0 the subsonic solutions must hit the sonic surface in $(x,S,\dot{S})$ space, since the solution with $A_0=0$ does, and regular solutions must hit it on the line Q. However, the behavior of the subsonic solutions is more complicated than that of the supersonic ones. This is illustrated by the lower part of Fig. 2, where the curves are labeled by the value of A_0. As the parameter A_0 decreases from positive values to some critical negative value A_0^{crit}, z_s decreases continuously to z_1. In this parameter range the solutions with $z_s>z_3$ are regular at the sonic point, while those with $z_1<z_s<z_3$ are all irregular. (The figure assumes $\alpha=1/3$, in which case $z_3=z_F$, so one has a continuous family of underdense solutions but no overdense solutions within this range; for other values of α, some of the overdense solutions are also in the continuous range.) As A_0 decreases below A_0^{crit}, the $V(z)$ curves develop an inflexion and z_s increases again to the value z_2. The subsonic solutions thus cross over each other in $V(z)$ space. Although one does not reach every value of z_s between z_1 and z_2, there is a band of solutions within $z_1<z<z_2$ which are regular (C^1) at the sonic point. This corresponds to the first band of overdense solutions and is associated with just a small range of A_0 values.

As A_0 decreases further, z_s moves back and forth between the values z_1 and z_2 and the $V(z)$ curves exhibit an increasing number of oscillations, although this is not shown in Fig. 2. One can group these solutions into families according to the number of oscillations they exhibit. Each family contains just a narrow band of solutions which are regular (C^1) at the sonic point and only one of these will be analytic there. This band structure also arises in the Newtonian situation [40]. It is possible that the non-analytic solutions are all unstable to what is termed the ''kink'' instability and form shocks [41]. Note that all the overdense solutions are nearly static close to the sonic point ($z_2=z_S$ if $\alpha=1/3$), although they deviate from the static solution as they go towards the origin. As the number of oscillations increases, the static solution remains a good approximation ever closer to the origin.

Provided there are points on Q which are intersected by solutions which are asymptotically Friedmann at both large and small z, one can construct a solution with a sound-wave which represents a density perturbation growing at the same rate as the Universe. As discussed in Sec. IV A, one would expect this to be possible providing there is a 1-parameter family of solutions at the sonic point, i.e. providing z_s lies in the range of values between z_1 and z_2 and above z_3. For in this case, for each point on Q, one would expect at least one supersonic solution to be asymptotically Friedmann and at least one subsonic solution to be regular at the origin. Furthermore, one would expect the value of $\dot{A}$ (corresponding to the density gradient or velocity gradient) to be continuous at the sonic point in such solutions, since only one value corresponds to the 1-parameter family. Numerical calculations [29] for the $\alpha=1/3$ case show that transonic solutions do indeed exist and have the features anticipated, although they do not span the entire range of values $z_1<z_s<z_2$. Note that, for each α, there is one asymptotically Friedmann supersonic solution which can be attached to the exact static solution inside the sonic point; this is just the solution for which z_s equals the value z_S given by Eq. (4.3). Likewise there is one asymptotically Friedmann subsonic solution which can be attached to the exact static solution outside the sonic point.

The form of $S(z)$ for these solutions is indicated in Fig. 3(a), the directions of the arrows corresponding to inceasing time, and is very similar qualitatively to the dust case [cf. Fig. 1(a) of Ref. [13]]. The curves are labeled by the value of the asymptotic energy E, where the special (negative) values E_* and E_{crit} are related to B_∞ and B_{crit} by Eq. (4.10). The $z>0$ solutions correspond to models which start from an initial big bang singularity at $z=\infty$ $(t=0)$ and then either expand to infinity as $z\to 0$ $(t\to\infty)$ for $E>E_{crit}$ or recollapse to a black hole at some non-zero value of z for $E<E_{crit}$. The ever-expanding solutions may be either underdense (for $E>0$) or overdense (for $E_{crit}<E<0$). The underdense ones and (for $\alpha\neq 1/3$) some of the overdense ones form a continuum, while the rest of the overdense family correspond to E lying in narrow bands between E_{crit} and 0. The figure indicates that the analysis is trivially extended to the $z<0$ regime. For since r is always taken to be positive, the $z<0$ solutions are just the time-reverse of the $z>0$ ones, so the solutions are symmetric in z. Thus the $E>E_{crit}$ models collapse from an infinitely dispersed initial state to a big crunch singularity as z decreases from 0 to $-\infty$ (i.e., as t increases

from $-\infty$ to 0), while the $E<E_{crit}$ models emerge from a white hole and are never infinitely dispersed.

Figure 3(b) shows the form of V(z) in these solutions but without giving any of the oscillations or fine structure in the subsonic sonic region [cf. Fig. 2]. In the $z>0$ regime, V either decreases monotonically towards 0 as z decreases or reaches a minimum and then increases to infinity at the singularity. The recollapsing solutions contain a black hole event horizon and a cosmological particle horizon for values of E exceeding the critical value E_*. Note that the last black hole solution (i.e. the one with the smallest z_S) is the one for which the minimum value of V reaches $1/\sqrt{\alpha}$ and this must touch the sonic surface at the value of z associated with the saddle/node transition (z_1). Figure 3(b) is similar to the equivalent figure in the dust case [cf. Fig. 1(b) of Ref. [13]], except that there are then no sonic points and no overdense ever-expanding solutions (essentially because $E_{crit}=0$ if $\alpha=0$).

C. Asymptotically Kantowski-Sachs solutions

If we wish to consider solutions which are asymptotic to the self-similar KS model, then Eq. (3.19) suggests that we introduce functions $A(z)$ and $B(z)$ defined by

$$x=x_0 z^{-2\alpha/(1+\alpha)}e^A, \quad S=S_0 z^{-1}e^B, \tag{4.14}$$

where x_0 and S_0 are given by Eq. (3.18) and z is taken to be positive. Following the analysis of Carr and Koutras [33], we linearize the equations in A, $\dot{A}$ and $\dot{B}$ to find the 1st order solution as $|V|\to\infty$. (Recall that V can be negative for the KS solution.) Equations (2.15) and (2.16) then yield

$$\ddot{B}=-\dot{A}+\left(\frac{1+3\alpha}{1+\alpha}\right)\dot{B}, \tag{4.15}$$

$$\dot{B}=\left(\frac{1}{2\alpha}\right)\dot{A}+\left(\frac{1-\alpha}{1+\alpha}\right)A. \tag{4.16}$$

If we differentiate the second equation and then substitute for $\dot{B}$ using the first, one obtains the following differential equation for A:

$$\ddot{A}+\left(\frac{\alpha-1}{\alpha+1}\right)\dot{A}-\frac{2\alpha(1+3\alpha)(1-\alpha)}{(1+\alpha)^2}A=0. \tag{4.17}$$

This has two solutions: $A\propto z^{-p_1}$ and $A\propto z^{-p_2}$ where

$$p_{1,2}=\frac{-1+\alpha\pm\sqrt{(1-\alpha)(24\alpha^2+7\alpha+1)}}{2(1+\alpha)}. \tag{4.18}$$

For $\alpha>0$, the KS solution has $|V|\to\infty$ as $z\to\infty$, so we must choose the positive root p_1. The general solution then has the form

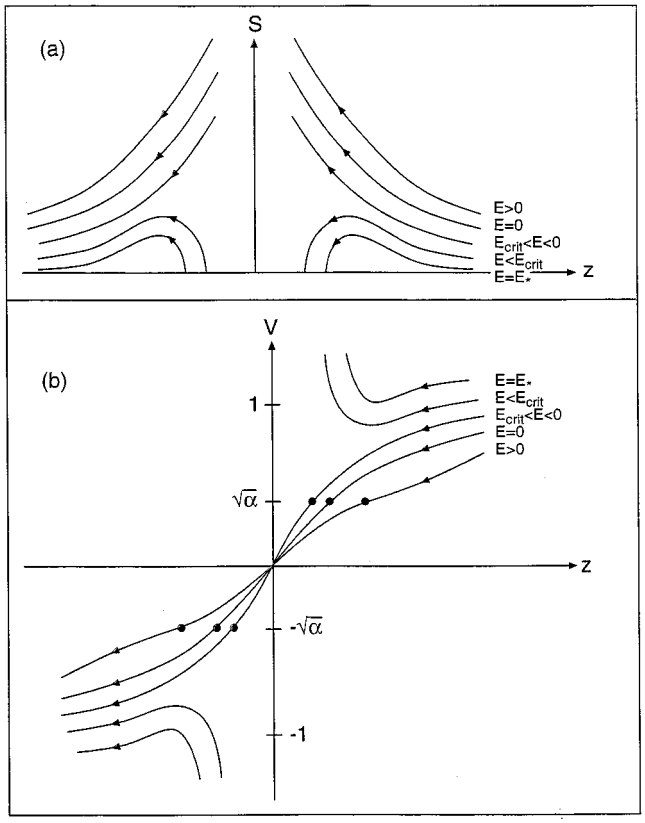

FIG. 3. This shows the form of the scale factor $S(z)$ and the velocity function $V(z)$ for the asymptotically Friedmann solutions with different values of E. The $z>0$ solutions expand from an initial singularity at $z=\infty$ and then either expand forever if $E>E_{crit}$ or recollapse to another singularity if $E<E_{crit}$. In the first case, the solutions necessarily pass through a sonic point [shown bold in (b)] and reach the origin. In the second case, they contain a black hole and a central singularity; there is an event horizon and particle horizon for $E_*<E<E_{crit}$. The $z<0$ solutions are the time reverse of the $z>0$ ones.

$$A=A_\infty z^{-p_1}, \quad B=A_\infty\left[\frac{1}{2\alpha}-\left(\frac{1-\alpha}{1+\alpha}\right)\frac{1}{p_1}\right]z^{-p_1} \tag{4.19}$$

where A_∞ is an integration constant. Although the expression for B could contain another integration constant, Eqs. (2.17) and (2.18) show that this must be zero. For $-1<\alpha<-1/3$, the KS solution has $|V|\to\infty$ as $z\to 0$, so we must choose a negative root in Eq. (4.18). Only p_2 is negative for this range of α, so this gives a solution like Eq. (4.19) but with p_2 replacing p_1. In both cases there is thus a 1-parameter family of asymptotically KS solutions. For $-1/3<\alpha<0$, one again has $|V|\to\infty$ as $z\to\infty$ but both p_1 and p_2 are negative, so there is no solution as $z\to\infty$. Since Eq. (3.31) shows that KS solutions with $-1/3<\alpha<0$ correspond to static solutions with $0<\alpha<1$ if r and t are interchanged (so that z goes to $1/z$), this is related to the fact that there are no asymptotically static solutions as $z\to 0$ for $0<\alpha<1$. In all cases, Eq. (2.21) implies that $\mathcal{E}\to -1/2$ as $z\to\infty$, so these are in some sense ''minimal energy'' solutions.

At small values of $|V|$, corresponding to small values of z for $\alpha>0$, Eqs. (2.17) and (2.18) imply that the A and B must tend to constants which are related by

$$e^{2B_0}=\frac{1}{2}\left[M_{KS}e^{-A_0(1+\alpha)/\alpha}-\left(M_{KS}-\frac{1}{2}\right)e^{-2A_0}\right]^{-1}, \tag{4.20}$$

where M_{KS} is defined by Eq. (3.23). This derives from the condition $\dot{A}=\dot{B}=0$ at $z=0$. There is thus a 1-parameter family of solutions and we can take this parameter to be A_0, which is a measure of the underdensity or overdensity at the origin relative to the exact KS solution. One can show there are only isolated solutions at a sonic point for $\alpha>0$ [33], so the parameter-counting argument given in Sec. IV A implies that any asymptotically KS solution which hits the sonic surface is unlikely to be regular there. For $0>\alpha>-1/3$, there is a 2-parameter family of solutions as $z\to 0$, related to the 2-parameter family of asymptotically quasi-static solutions with $1>\alpha>0$ as $z\to\infty$. For $-1<\alpha<-1/3$, $V\to 0$ as $z\to\infty$ and there is again a 1-parameter family of solutions.

Henceforth we will focus on the $\alpha>0$ solutions. The physical significance of these solutions is unclear, so we do not present the $S(z)$ plot. However, Carr and Koutras have integrated the equations in the $\alpha=1/3$ case and Fig. 6 reproduces the $V(z)$ curves corresponding to different values of the asymptotic parameters A_∞ and A_0. Note that Eq. (3.31) shows that these solutions are related to asymptotically static ones with $\alpha=-1/5$ but these solutions are also unphysical since they have negative mass from Eq. (3.29). Although they did not attempt to explain any features of these solutions, we can now do so by invoking the results of Sec. III.

Let us first consider the *supersonic* solutions with $V<-\sqrt{\alpha}$. The underdense ones have A_∞ positive. As z decreases from infinity, they all cross $V=-1$ at some point to the left of the exact KS solution. However, they do not hit the sonic point but reach a maximum between $V=-\sqrt{\alpha}$ and $V=-1$ as z decreases. They then hit the $V=-1$ surface again (all with $\dot{V}=1$ and the same value of z), with M and μ tending to zero and the scale factor S diverging. This behavior is analogous to that which arises for the solutions which are asymptotically Minkowski at finite z. The overdense supersonic solutions have A_∞ negative and, as z decreases, they all hit the sonic line to the right of the exact KS solution. As A_∞ decreases, the point at which they hit the sonic line moves to infinity. All the supersonic solutions have $M<0$ everywhere and so never cross the $M=0$ curve in Fig. 1(b). As $z\to\infty$, both A and B go to 0, so V tends to the exact KS form.

Let us now consider the *subsonic* solutions with $0>V>-\sqrt{\alpha}$. The overdense ones have A_0 negative. None of them hit the sonic surface since they reach a minimum as z decreases and then asymptotically approach $V=0$. The interesting feature of these solutions is that the function M, which is negative at the origin, goes through zero and becomes positive as z increases. This is because these solutions cross the curve given by Eq. (3.45) in $V(z)$ space; they eventually cross this curve again but without the sign of M reversing. M and μr^2 tend to infinity as $z\to\infty$. The asymptotic behavior of these solutions is described by Eqs. (3.32) to (3.34). The underdense solutions have A_0 positive and hit the sonic line to the left of KS.

D. Asymptotically quasi-static solutions

If we wish to consider $(z>0)$ solutions which are asymptotically static, we introduce functions $A(z)$ and $B(z)$ defined by

$$x=x_o e^A, \quad S=S_o e^B \tag{4.21}$$

where x_o and S_o are given by Eq. (3.30). We initially assume $z>0$, although we will eventually need to extend the solutions into the $z<0$ regime. Equations (2.15) and (2.16) then become

$$\ddot{B}+3\dot{B}^2-\frac{\dot{A}}{\alpha}+\left(\frac{\alpha+3}{\alpha+1}\right)\dot{B}-\left(\frac{1+\alpha}{\alpha}\right)\dot{A}\dot{B}=0 \tag{4.22}$$

$$V^2\left(\dot{B}-\frac{\dot{A}}{2\alpha}\right)=-\frac{\dot{A}}{2}+\left(\frac{\alpha}{1+\alpha}\right)[e^{-4B+A(1-\alpha)/\alpha}-1]. \tag{4.23}$$

To find the first order solution as $V\to\infty$ (i.e. as $z\to\infty$), we linearize these equations to obtain

$$\ddot{B}=\frac{\dot{A}}{\alpha}-\left(\frac{\alpha+3}{\alpha+1}\right)\dot{B} \tag{4.24}$$

$$\dot{B}=\dot{A}/(2\alpha), \tag{4.25}$$

where the second equation is required since both sides of Eq. (4.23) must be finite as $V\to\infty$. Eliminating $\dot{A}$ gives

$$\ddot{B}+\left(\frac{1-\alpha}{1+\alpha}\right)\dot{B}=0 \tag{4.26}$$

and this leads to the general solution

$$A=A_\infty+Cz^{-(1-\alpha)/(1+\alpha)}, \quad B=B_\infty+\left(\frac{C}{2\alpha}\right)z^{-(1-\alpha)/(1+\alpha)}, \tag{4.27}$$

where A_∞, B_∞ and C are integration constants. Equations (2.17) and (2.18) give another relationship between these constants:

$$C\sim\left[e^{2B_\infty-(1+\alpha)A_\infty/\alpha}-\left(\frac{1+6\alpha+\alpha^2}{4\alpha}\right)+\frac{(1+\alpha)^2}{4\alpha}e^{6B_\infty-2A_\infty/\alpha}\right]^{1/2}e^{A_\infty-B_\infty} \tag{4.28}$$

where we have omitted a coefficient which depends on α. This shows that the asymptotically static solutions are described by two parameters for a given equation of state. A_∞ gives the asymptotic density perturbation relative to the exact static solution, this being positive (negative) for underdense (overdense) solutions; B_∞ gives the asymptotic value

of the scale factor relative to its value in the exact static solution. Since the square root in Eq. (4.28) can have either sign, there will be two solutions for a given value of B_∞, with different signs for $\dot{B}$.

It should be stressed that the description ''asymptotically static'' in this context is rather misleading. This is because Eqs. (2.20) and (4.27) imply

$$V_R \approx -\frac{(1-\alpha)}{2\alpha(1+\alpha)}C \tag{4.29}$$

at large z, so in general solutions will be either expanding (for $C>0$) or collapsing (for $C<0$). Only the 1-parameter family of solutions with $C=0$ are asymptotically static in the sense that the fluid is not moving with respect to the spheres of constant R. This agrees with the description of Foglizzo and Henriksen [36], who term such solutions ''symmetric.'' The *exact* static solution has $A_\infty=B_\infty=C=0$. We will describe the more general 2-parameter solutions with $C\neq 0$ as asymptotically ''quasi-static:'' Eq. (4.27) implies that these solutions have both dS/dz and zdS/dz going to zero at infinity, as in the dust case, but z^2dS/dz scales as $z^{2\alpha/(1+\alpha)}$ and therefore diverges rather than tending to a finite value. These solutions also exhibit an isothermal density profile at large z in the sense that μr^2 is constant.

The behavior of the asymptotically quasi-static solutions at large z is analogous to that found in the dust case, where the solutions are also described by two parameters. The first one relates to the asymptotic energy E. At large values of z, Eq. (2.20) implies that the energy function is

$$\mathcal{E}=\frac{(1+\alpha)^2}{2(1+6\alpha+\alpha^2)}e^{6B_\infty-2A_\infty/\alpha} \times\left[1-\frac{C(3-\alpha)}{\alpha(1+\alpha)}z^{-(1-\alpha)/(1+\alpha)}\right]-\frac{1}{2}, \tag{4.30}$$

where we have used Eq. (4.27), so we infer

$$E=\frac{(1+\alpha)^2}{2(1+6\alpha+\alpha^2)}e^{6B_\infty-2A_\infty/\alpha}-\frac{1}{2}. \tag{4.31}$$

In the dust case, the second parameter corresponds to the value of z associated with the big bang or big crunch singularity (viz. $|z|=1/D$) and we will use a similar characterization in the general α case. However, it should be stressed that this value can only be determined numerically if there is pressure and so cannot be expressed in terms of A_∞ and B_∞ explicitly. It is therefore convenient to also associate the second parameter with the asymptotic value of V_R, given in terms of C by Eq. (4.29). This has the advantage that (like E) it can be expressed explicitly in terms of A_∞ and B_∞ from Eq. (4.28), although the expression is complicated. The parameter C is only implicitly related to the parameter D.

One of the differences from the dust case is that there is now an *exact* static solution with $A_\infty=B_\infty=0$. In this case, $\mathcal{E}$ is just $-M$ from Eq. (2.22), where M is given by Eq. (3.29), and so

$$\mathcal{E}=E_{stat}\equiv-\frac{2\alpha}{1+6\alpha+\alpha^2}. \tag{4.32}$$

This can also be seen directly from Eq. (4.31). However, one requires an infinite value for D in the exact static solution, so that the central singularity is at $z=0$. From Eq. (4.31) there is also a 1-parameter family of solutions which have this energy asymptotically and they must satisfy the condition

$$B_\infty=A_\infty/3\alpha \quad (E=E_{stat}). \tag{4.33}$$

For comparison, Eq. (4.31) shows that the 1-parameter family of solutions with zero asymptotic energy must have

$$B_\infty=\frac{1}{3\alpha}A_\infty+\frac{1}{6}\ln\left[\frac{1+6\alpha+\alpha^2}{(1+\alpha)^2}\right] \quad (E=0). \tag{4.34}$$

Two more interesting 1-parameter families can be defined. Equations (2.19) and (4.21) imply that the asymptotic velocity is the same as in the exact static case for solutions with

$$B_\infty=\left(\frac{2\alpha}{1-\alpha}\right)A_\infty. \tag{4.35}$$

For $\alpha=1/3$, this happens to coincide with condition (4.33). From Eq. (4.28) the condition $C=0$ defines another more complicated relationship:

$$B_\infty=\left(\frac{1-\alpha}{4\alpha}\right)A_\infty+\frac{1}{2}\ln\sinh\left[\frac{1}{3}\sinh^{-1}k_1\exp\left(\frac{1+3\alpha}{2\alpha}A_\infty\right)\right]+k_2 \tag{4.36}$$

where k_1 and k_2 are α-dependent constants. This corresponds to the subset of *symmetric* solutions and is also associated with a D-dependent asymptotic energy $E_{sym}(D)$. For large positive values of A_∞ and B_∞, Eq. (4.36) reduces to the condition $E=0$ given by Eq. (4.34). For large negative values of A_∞ and B_∞, it reduces to

$$B_\infty=\left(\frac{1+\alpha}{2\alpha}\right)A_\infty+\frac{1}{2}\ln\left[\frac{1+6\alpha+\alpha^2}{4\alpha}\right]. \tag{4.37}$$

Equation (4.36) also specifies a lower limit on B_∞, and hence S_∞, since Eq. (4.28) would not give a real value for C if it was less than this.

To find asymptotically static solutions at small values of z, one seeks solutions with $V=0$ and finite values of A and B at $z=0$. [Equation (2.20) implies that such solutions necessarily have $V_R=0$.] However, this requires $\dot{A}=\dot{B}=0$, which from Eq. (4.23) implies

$$4B_o=\left(\frac{1-\alpha}{\alpha}\right)A_o. \tag{4.38}$$

It is easy to see that this condition is incompatible with Eqs. (2.17) and (2.18) unless $A_o=B_o=0$, so there are no asymptotically static solutions at $z=0$ (only the exact static solution itself). If instead we seek solutions in which $V=0$ and $\dot{A}$

and $\dot{B}$ are finite and non-zero at $z=0$, so that A and B diverge logarithmically, then Eq. (4.23) implies

$$\dot{A}=-\left(\frac{2\alpha}{1+\alpha}\right). \tag{4.39}$$

Substituting this into Eq. (4.22) gives

$$3(1+\alpha)\dot{B}^2+(5+3\alpha)\dot{B}+2=0, \tag{4.40}$$

which has the two roots

$$\dot{B}=-\frac{2}{3(1+\alpha)} \quad \text{or} \quad \dot{B}=-1. \tag{4.41}$$

However, these roots just correspond to solutions which are asymptotically Friedmann or asymptotically Kantowski-Sachs at $z=0$ and we analyzed such solutions in the previous sections.

To understand the physical interpretation of the asymptotically quasi-static solutions, one must extend the above analysis to the $z<0$ regime and consider the form of the function $S(z)$. As illustrated in Fig. 4(a), this form is very similar to the dust case [cf. Fig. 3(a) of Ref. [13]], with the solutions necessarily spanning both positive and negative values of z. All the solid curves correspond to cosmological models which start off expanding from a big bang singularity at $z=-1/D$, then tend to the asymptotically quasi-static form as $z\to-\infty$ and then cross over to $z=+\infty$. They then either expand forever (upper two curves) if E exceeds some negative critical value $E_{crit}(D)$ or recollapse (lower two curves) if E is less than $E_{crit}(D)$. In the latter case the solution contains a black hole and a second singularity at $z=z_S$. The singularity forms with zero mass at $t=0$ but its mass $m_S=(MSz)_S t$ then grows as t. As in the dust case, the value of z at the second singularity is necessarily less than $1/D$ and S always has a maximum in $z>0$. The broken curves are the time reverse of the solid ones and correspond to cosmological models which all collapse to a big crunch singularity at $z=+1/D$ but may start off either expanding from a white hole or collapsing from infinity. For the symmetric solutions with $E=E_{sym}$, $z_S=1/D$ and the solid and broken curves coincide.

Note that the $z<0$ solutions can be obtained from the $z>0$ ones by reflection, so either side of Fig. 4(a) gives complete information about the solutions. However, one needs both sides to track a particular solution. The fact that there are two curves for each asymptotic value of S is a consequence of Eq. (4.28) giving two values for dS/dz: as in the dust case, the solid one has a negative gradient, while the dotted one has a positive gradient, and a given solution must preserve its gradient as it goes from $z=-\infty$ to $z=+\infty$. The form of the solution near either $|z|=1/D$ or $|z|=z_S$ is given by Eq. (3.64) but (unlike the asymptotic Friedmann case) one now needs the full 1-parameter family of solutions for given z_S since the asymptotically quasi-static solutions are described by two parameters.

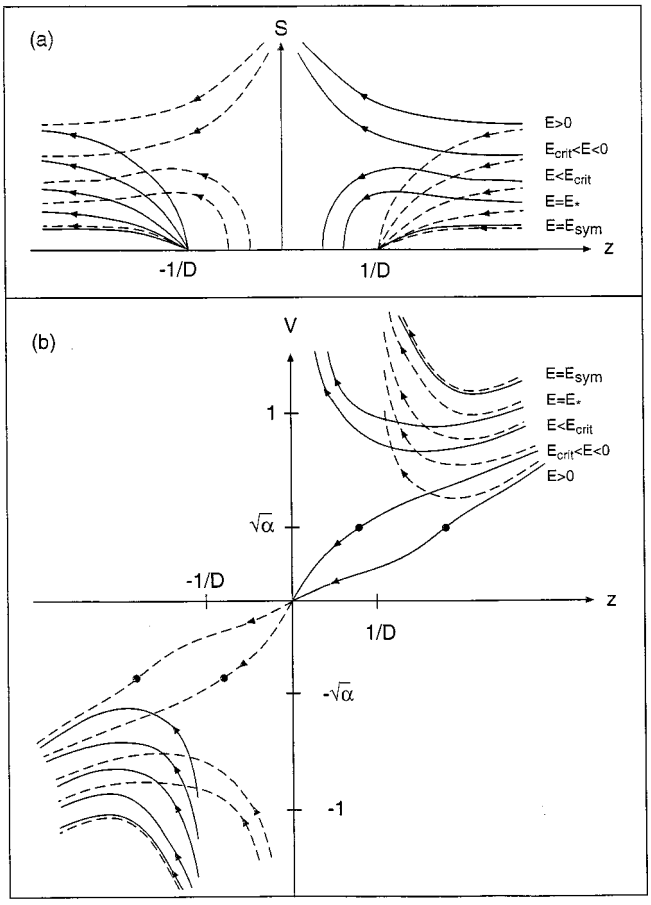

FIG. 4. This shows the form of the scale factor $S(z)$ and the velocity function $V(z)$ for the asymptotically quasi-static solutions with different values of E but fixed D. The solutions necessarily span both positive and negative z. The solid curves show solutions which expand from an initial singularity at $z=-1/D$ and then either expand forever if $E>E_{crit}(D)$, in which case they pass through a sonic point [shown bold in (b)], or recollapse to another singularity if $E<E_{crit}(D)$. There is an event horizon and particle horizon for $E_*(D)<E<E_{crit}(D)$. The last recollapsing solution is the symmetric one for which $E=E_{sym}$. The broken curves are the time reverse of the solid ones. These all collapse to a final singularity at $z=1/D$ and this is naked for E less than some value $E_+(D)$, which may be negative or positive but necessarily exceeds the value $E_{crit}(D)$.

The form of $V(z)$ in these solutions is indicated in Fig. 4(b) and is also similar to the dust case except that there are now sonic points. The ever-collapsing solutions start with $V=0$ at $z=0$ and then, as z decreases, pass through a sonic point (where $V=-\sqrt{\alpha}$) and then a Cauchy horizon (where $V=-1$) before tending to the quasi-static form at $z=-\infty$. They then jump to $z=+\infty$ and enter the $z>0$ regime. As z further decreases, V first reaches a minimum and then diverges when it encounters the big crunch singularity at $z=1/D$. As in the dust case, the minimum of V will be above or below 1 according to whether E is more or less than some value $E_+(D)$ and one necessarily has a naked singularity in the latter case [see Fig. 16 in Ref. [19]]. If the minimum of V were less than $\sqrt{\alpha}$, the collapsing solutions would need to

have two sonic points in the $z>0$ regime. However, it is unlikely that such solutions would be regular at the second sonic point, so one would expect collapsing solutions to exist only for values of the parameters such that the minimum of V exceeds $\sqrt{\alpha}$. This applies providing E is less another critical value which is necessarily less than $E_+(D)$. The ever-expanding solutions are just the time reverse of the ever-collapsing ones.

The form of $V(z)$ for the expanding-recollapsing solutions, which arise if $E<E_{crit}(D)$, is also indicated in Fig. 4(b). There are two solutions of this kind. In one (solid) V starts off at $-\infty$ when $z=-1/D$, rises to a maximum, then falls off asymptotically quasi-statically as $z\rightarrow-\infty$, then jumps to $z=+\infty$ and then falls to a minimum before rising to $+\infty$ at $z=z_S$. [For the reasons indicated above, it is likely that the maximum is less than $-\sqrt{\alpha}$ and that the minimum is more than $+\sqrt{\alpha}$, in which case these solutions have no sonic points.] The minimum will be less than 1 if E exceeds the value $E_*(D)$ and the maximum will exceed -1 if E is less than the value $E_+(D)$. In the first case, one has a black hole event horizon and a cosmological particle horizon. The other kind of expanding-recollapsing solution (broken) is the time reverse of this and goes from $z=-z_S$ to $z=1/D$. In this case one has a naked singularity at $z=1/D$ if $E<E_+(D)$.

Since the minimum of the solid curve in Fig. 4(b) is always below the minimum of the broken curve for a given value of S_∞, we infer that there are recollapsing solutions which have an event horizon in $z>0$ without having a naked singularity in $z<0$. Likewise there are solutions with $0>E>E_{crit}(D)$ which have a sonic point in $z>0$ without having one in $z<0$. However, if E is sufficiently larger than $E_{crit}(D)$, there might also be solutions in which *both* the solid and broken curves have a sonic point. This would correspond to bouncing solutions (with two sonic points but no singularities), in which S starts off decreasing and ends up increasing. In these solutions V would decrease monotonically from $z=0^-$ to $z=-\infty$ and then from $z=+\infty$ to $z=0^+$. However, we have seen that it is unlikely that such solutions could exist since they would require two regular sonic points.

We note that although the introduction of the parameter D has a crucial effect in the large-$|z|$ regime, changing the solution from the asymptotically Friedmann to asymptotically quasi-static form, it has relatively little effect in the subsonic regime. One can therefore still use the results of the asymptotically Friedmann analysis here (at least qualitatively). In particular, one still has oscillations — though none of these are shown in Fig. 4(b)—and the model can only collapse from infinity if E is positive or lies in discrete bands if negative. The main difference is that the sonic point may now be a saddle rather than a node. However, in this case, we saw in Sec. IV A that the subsonic solution is unlikely to reach $z=0$.

Some of the asymptotically quasi-static similarity solutions with pressure have already been studied numerically by Foglizzo and Henriksen [36], although they only focus on the collapsing solutions. (The relationship between their variables and ours is given in Appendix B.) They confirm many of the qualitative features described above. In particular, they show that the solutions are described by two parameters at large $|z|$ and by one parameter at small $|z|$ and they find the expected behavior at the sonic point. In their phase space analysis, the orbits corresponding to the overdense solutions converge on and then spiral around the static solution for a while before heading to the origin. This corresponds to the oscillations discussed in Sec. IV B, with the number of oscillations identifying the overdensity band. Foglizzo and Henriksen confirm that the solutions with $V_{min}<1$ exhibit naked singularities. Indeed, the static attractor is closely related to the self-similar solutions which arise in critical phenomena [8]. This is discussed in more detail by Carr and Henriksen [42].

E. Asymptotically Minkowski solutions

The asymptotically Minkowski solutions cannot be analyzed in the same way as the other solutions discussed above since the limiting solution is not itself self-similar. Thus in seeking the various asymptotic forms, one cannot perturb about an exact background self-similar solution. Also one cannot analyze these solutions in terms of the parameter E since the energy function asymptotically diverges, Eqs. (2.21), (3.37) and (3.52) implying

$$\mathcal{E}\sim\left|\ln|z/z_*|\right|^{4\alpha/(1-5\alpha)},\quad \mathcal{E}\sim z^{2V_*/(V_*^2-1)} \tag{4.42}$$

for the two families. (We use double modulus signs in the first expression since we now allow z to be negative and the logarithm may also be negative.) Nevertheless one can still use the considerations of Sec. III to derive the forms of $S(z)$ and $V(z)$ for these solutions and these are indicated in Figs. 5(a) and 5(b). For the solutions which asymptote to infinite $|z|$ and are described by one parameter, Eqs. (3.37) and (3.42) apply; for the ones which asymptote to z_* and are described by two parameters, Eqs. (3.52) and (3.57) apply. Figure 5(a) shows that all the $z>0$ solutions start off collapsing at large distances (be this at infinite or finite z) and then either collapse to a singularity at z_S or bounce into an expansion phase. The $z<0$ solutions are just the time reverse of these. In deriving the form of $V(z)$ shown in Fig. 5(b), we use Eq. (3.57). Although these solutions represent a large fraction of the complete solution space, many of their features are still unexplored.

F. Complete solution space

The form of the function $V(z)$ for all the $z>0$ solutions is brought together in Fig. 6 for the $\alpha=1/3$ case. Similar figures could be presented for $\alpha>1/3$ and $\alpha<1/3$ but these are not shown explicitly. The equations simplify in the $\alpha=1/3$ case, so this is the one which has been most studied numerically. Also this is the case likely to apply in the early universe. Although the $V(z)$ diagram does not give complete information about the solution space, since this is

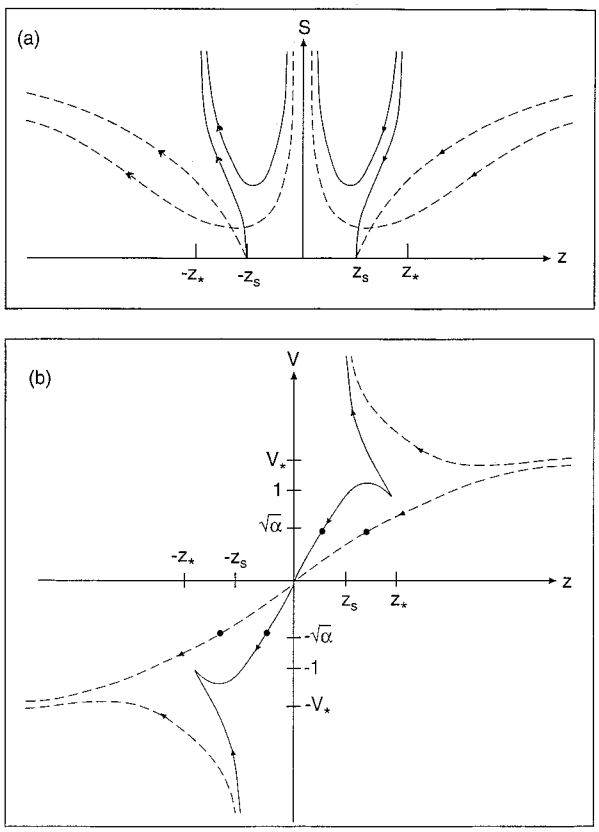

FIG. 5. This shows the form of the scale factor $S(z)$ and the velocity function $V(z)$ for the asymptotically Minkowski solutions, which exist only for $\alpha>1/5$. One family (solid lines) asymptotes to the finite value z_* with $V\to 1$; the other family (broken lines) asymptotes to infinite z with $V\to V_*>1$. In both cases, there are solutions which collapse monotonically to a central singularity (z_S) and solutions which collapse and then bounce into an expansion phase; the latter necessarily have a sonic point [shown bold in (b)]. The $z<0$ solutions are the time reverse of these.

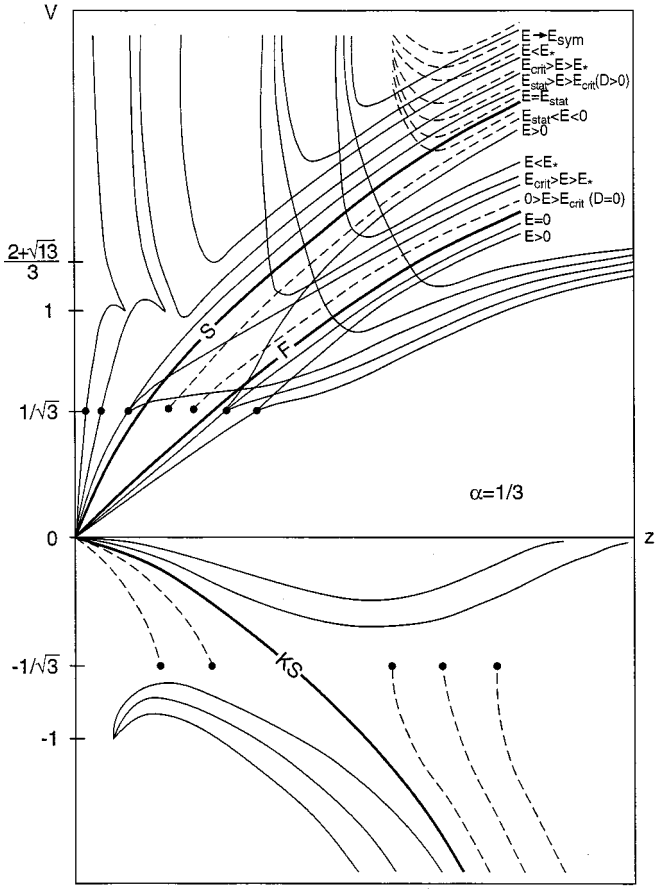

FIG. 6. This shows the form of the velocity function $V(z)$ for the full family of spherically symmetric similarity solutions with $\alpha=1/3$. The exact Friedmann, Kantowski-Sachs and static solutions are indicated by the bold lines. Also shown are the asymptotically Friedmann solutions (for different values of E), the asymptotically quasi-static solutions (for different values of E and fixed D) and the solutions which are asymptotically Minkowski at finite or infinite z. The broken curves give the extrapolation of the asymptotically quasi-static solutions into the $z<0$ regime and all asymptote to infinity at $z=1/D$. Solutions shown by dashed lines are irregular at the sonic point (shown bold) and cannot be extended beyond there. All the other solutions are either supersonic everywhere or C^1 at the sonic point. Solutions which are analytic at the sonic point form just a small subset of the latter. The negative V region is occupied by the asymptotically Kankowski-Sachs solutions, although these may not be physical since the mass is negative. For a full description of these solutions, see the discussion in Sec. IV F.

3-dimensional, it does convey many important physical features of the solutions (in particular, the occurrence of singularities and event horizons). Other interesting physical quantities, such as the density μ and the mass function M, are discussed in Ref. [10].

It should be emphasized that Fig. 6 is only qualitative and does not include fine details, such as the oscillations in the subsonic regime. In order to avoid the figure being too cluttered, only a few members of each family are shown and we do not include solutions which are non-physical in the subsonic regime. However, we do include some solutions which terminate at the sonic point and these are shown by dashed lines. The figure only shows the positive z regime but this still gives complete information. The solutions are labeled by their asymptotic energy E whenever this is well defined.

The form of $V(z)$ for the asymptotically Friedmann solutions (with $D=0$) comes directly from Fig. 3(b), with the significance of the energies E_* and E_{crit} being described in Sec. IV B. Two recollapsing solutions are shown (one of which contains an event horizon and a particle horizon), one regular and one irregular overdense solution, and two regular underdense solutions. For a general value of α, it should be noted that Eqs. (2.19), (4.1), (4.8) and (4.12) give the asymptotic velocity as

$$V\approx e^{(1-3\alpha)A_o/\alpha}V_F \quad (z\ll 1), \quad V\approx e^{-2B_\infty}V_F \quad (z\gg 1) \tag{4.43}$$

where V_F is the exact Friedmann velocity. For $\alpha>1/3$, V is more (less) than V_F for the overdense (underdense) solutions at all values of z. However, for $\alpha<1/3$, V starts below (above) V_F at small z and ends up above (below) it at large z

for the overdense (underdense) solutions. In this case, the solutions cross over each other, which makes the $V(z)$ diagram rather complicated. For $\alpha=1/3$, the dependence of V upon A_o at small z only appears at second order and so such criss-crossing is avoided.

The form of $V(z)$ for the asymptotically quasi-static solutions is taken from Fig. 4(b), except that both quadrants are now folded into $z>0$. The solid curves come from the upper right quadrant in Fig. 4(b) and the broken ones from the lower left quadrant. Thus the latter can be regarded as the extrapolation into the $z<0$ regime of the former. All the solutions have the same value of D, so all the broken lines asymptote to infinity at $z=1/D$, but they have different values of E. It should be stressed that the values of E_* and E_{crit} depend on D and therefore differ from the corresponding values for the asymptotically Friedmann solution. Equation (4.32) implies that the value of E for the exact static solution (which can be regarded as the limit of the symmetric solution as $D\to\infty$) is $E_{stat}=-3/14$ for $\alpha=1/3$. From Eqs. (4.33) and (4.35) the velocity for all solutions with this energy asymptotes to the exact static form if $\alpha=1/3$ but this feature does not apply for other values of α. Besides the exact static solution, four recollapsing solutions are shown (one of which has an event horizon and particle horizon). There is one regular and one irregular solution which is overdense relative to Friedmann and one regular solution which is underdense.

The form of $V(z)$ for the asymptotically Kantowski-Sachs solutions is taken from Fig. 2 of Ref. [33]. Although the physical significance of these solutions is unclear since, for $\alpha=1/3$, the Kantowski-Sachs solution is tachyonic and has negative mass, their mathematical characteristics were explained in Sec. IV C. All the solutions which reach a sonic point are irregular there, as indicated by the dashed curves.

The form of $V(z)$ for the asymptotically Minkowski solutions is taken from Fig. 5(b), except that all the solutions are here represented by solid lines. Note that these solutions cannot be labeled by their asymptotic energy since, as indicated by Eq. (4.42), this diverges. Five of them are asymptotically Minkowski as $z\to\infty$, with V going to the value $V_*=(2+\sqrt{13})/3$ indicated by Eq. (3.42). Two of these collapse monotonically (one containing an event horizon and a particle horizon); the other three start off collapsing but then bounce into an expansion phase (one being overdense and the others underdense at the origin relative to Friedmann). The remaining solutions are asymptotically Minkowski at a finite value z_* and $V\to 1$ there. The upper parts of the curves correspond to solutions which collapse monotonically, while the lower parts correspond to solutions which collapse and then bounce. Examples of such solutions extend to higher values of z_* than indicated but are not shown to avoid cluttering.

It is interesting that the collapsing solutions which are asymptotic to either the Friedmann or Minkowski solutions as $z\to\infty$ have a minimum value of z_S (the value of z at the singularity) and this is the same in each case. This is because, for any 1-parameter solution, the last black hole solution is the one for which the minimum of V reaches $\sqrt{\alpha}$ and this must occur where the sonic point changes from a node to a saddle (i.e. at $z=z_1$). However, the value of z_S for the 2-parameter solutions can be arbitrarily small.

V. DISCUSSION

In this paper we have analyzed the complete family of spherically symmetric self-similar solutions for a perfect fluid with equation of state $p=\alpha\mu$. The key steps underlying our analysis are: (1) a delineation of the possible asymptotic forms at large and small distances from the origin; (2) an elucidation of the link between the $z>0$ and $z<0$ solutions; (3) an explicit use of the dust solutions (which can be expressed analytically) to understand heuristically various features of the solutions in the supersonic regime; and (4) a detailed analysis of solutions which are regular at the origin (i.e. asymptotically Friedmann as $r\to 0$ or $t\to\infty$) in order to understand solutions in the subsonic regime.

In claiming that our classification is ''complete,'' it should be emphasized that our considerations have been restricted in a number of ways. We plan to extend our analysis to avoid these restrictions in future work but for present purposes it will be useful to list them explicitly. Some of the restrictions could be regarded as geometrical and others as physical.

The first *geometrical* restriction is that we have confined attention to self-similar solutions of the ''first'' kind (i.e., homothetic solutions in which the similarity variable is $z\equiv r/t$). However, it may be possible to extend this work to the classification of self-similar solutions of the ''second'' kind. For example, in spherically symmetric perfect fluid solutions which possess kinematic self-similarity, the similarity variable is of the form $z=r/t^a$, where the exponent a depends on some dimensional constant which contains a scale [43]. There is evidence that such solutions asymptote towards exact solutions that admit a homothetic vector [44], so the asymptotic analysis in this paper may be of rather more general application than is at first apparent; i.e., the asymptotic behavior of *all* self-similar solutions (not only those of the first kind) may be determined by the solutions described in this paper. Of course, the behavior at *finite* values of the similarity variable, including for example the behavior at sonic points and horizons, may be quite different.

The second geometrical restriction is that we have assumed that the homothetic vector is neither parallel nor orthogonal to the fluid velocity. Although solutions with these properties do exist, they are not covered by the analysis of Sec. II. However, it can be shown that all perfect fluid spacetimes (not only spherically symmetric ones) admitting a homothetic vector parallel to the velocity vector are necessarily Friedmann [45]. In addition, it has claimed that all spherically symmetric spacetimes which admit a homothetic vector orthogonal to the velocity vector have a singular metric [46].

The main *physical* restriction is that we have confined attention to perfect fluids with a barotropic equation of state (necessarily of the form $p=\alpha\mu$) and so our analysis does not cover more general perfect fluids or anisotropic fluids, even though these may be of physical interest. In particular, a two-perfect-fluid model, in which each component is nec-

essarily comoving and has an equation of state of the form $p_i=\alpha_i\mu_i$ $(i=1,2)$, is formally equivalent to a single perfect fluid that does not have an equation of state. It is therefore plausible that perfect fluid models for which p/μ is asymptotically constant may have the same asymptotic behavior as the self-similar solutions studied in this paper. This is indeed the case for two-fluid models in which each component separately satisfies the conservation equations. This is discussed further in Appendix C.

Even within the context of fluids with $p=\alpha\mu$, we have not covered every possible value of α. In particular, we have not considered the stiff case $(\alpha=1)$, in which the speed of sound is equal to the speed of light. Since $\alpha=1$ is a bifurcation value, there can be significant changes in the qualitative behavior from the $\alpha<1$ case. Therefore a discussion of stiff perfect fluid solutions may be important in understanding the dynamics of the complete class of self-similar solutions. A partial analysis of the $\alpha=1$ case has been made by Lin et al. [27] and Bicknell and Henriksen [28]. However, if $\alpha=1$, Eq. (2.19) implies that V has no explicit dependence on z and, when $V\neq 1$, Eqs. (2.15) and (2.16) yield a single, second-order autonomous ordinary differential equation for S. This equation can be better studied using different mathematical techniques to those employed in this paper. In this context, it should be emphasized that our analysis does not cover the case in which the source is a massless scalar field since (if there is no scalar potential) this is formally equivalent to a stiff fluid whenever the gradient of the scalar field is timelike. The relevance of self-similar solutions to the occurrence of critical phenomena in scalar field collapse has been studied by many authors [8–10,42,47].

We have not considered solutions with $\alpha<0$, even though these may be physically interesting in some contexts [34]. Indeed the Kantowski-Sachs solutions may *only* be applicable in this context. In fact, the asymptotic analysis can be extended to the $\alpha<0$ case [20]. When $\alpha=-1$, the perfect fluid source is equivalent to a cosmological constant. In this case, a scale is introduced and so there are no self-similar solutions of the first kind. However, spherically symmetric self-similar solutions of the more general (second) kind are still possible [48].

Finally it should be stressed that we have not considered solutions with shocks (cf. [1]). However, these may certainly be of physical interest, especially since transonic solutions which are C^1 rather than C^∞ at the sonic point may evolve into shocks due to the ''kink'' instability [41]. Nor have we considered ''patched'' solutions which are only self-similar for some range of coordinates or in which the value of α is different in different regions.

ACKNOWLEDGMENTS

We thank Martin Goliath, Dick Henriksen, Ulf Nilsson and Claes Uggla for useful discussions and Andrew Whinnett for help with some numerical work. An earlier version of this paper omitted the asymptotically Minkowski solutions and we extended our analyis to cover these only after their existence was ascertained by Goliath, Nilsson and Uggla numerically. B.J.C. is grateful to the Department of Mathematics and Statistics at Dalhousie University and the Yukawa Institute for Theoretical Physics at Kyoto University for hospitality received during this work. A.A.C. is supported by the NSERC.

APPENDIX A

In this paper we have used ''comoving'' coordinates, since this approach is best suited to studying the solutions explicitly. However, it should be stressed that our work is complemented by the analysis of Bogoyavlenski [15] and Goliath et al. [17,18] using ''homothetic'' coordinates and that of Ori and Piran [19] and Maison [9] using Schwarzschild coordinates. In this appendix, we discuss these other approaches in more detail.

In the homothetic approach, the coordinates are adapted to the homothetic vector and this yields results which complement and, in some cases, provide more rigorous demonstrations of the conclusions reached in this paper. However, in the homothetic approach, spacetime must be covered by several coordinate patches, one in which the homothetic vector is spacelike and one in which it is timelike. These regions must then be joined by a surface in which the homothetic vector is null and this surface is associated with important physics. Bogoyavlenski [15] studied the spacelike and timelike cases simultaneously (with the metric being written in ''conformally static'' form) and continuously matched the two regions to obtain the behavior of solutions crossing the null surface. However, it should be noted that Bogoyavlenski changed comoving coordinates explicitly to describe the physics of the associated solutions.

Recently Goliath et al. [17,18] have reinvestigated both the spatially and temporally self-similar cases. The timelike region contains the more interesting physics (e.g. shocks and sound-waves). They introduce dimensionless variables, so that the number of equations in the coupled system of autonomous differential equations is reduced, with the resulting reduced phase space being compact and regular. In this way the similarities with the equations governing hypersurface orthogonal models, and in particular spatially homogeneous models [12,49], can be exploited. In their approach, all equilibrium points are hyperbolic, in contrast to the earlier work [15] in which non-compact variables were used, resulting in parts of phase space being ''crushed.''

The Schwarzschild approach is better suited to studying the causal structure of the self-similar solutions. This is because, in order to obtain physically reasonable models, spacetimes are often required to be asymptotically flat. Since asymptotically flat spacetimes are not self-similar, one therefore needs to match a self-similar interior region to an non-self-similar exterior region and this is usually taken to be Schwarzschild. In particular, Schwarzschild coordinates are most suitable for solving the equations of motion for (radial) null geodesics, as required in studying the global structure of the solution. Consequently it was used by Ori and Piran [19] since one of their primary goals was to study naked singularities and test the cosmic censorship hypothesis. However, the Schwarzschild coordinates break down at $t=0$.

APPENDIX B

The precise transformations between the various coordinate systems used to study self-similar spherically symmetric perfect fluid models are given explictly in Bogoyavlenski ([15]; see Sec. 3 of Chap. IV). The coordinate transformations between the comoving and Schwarzschild systems, both of which are employed by Ori and Piran [19], are given explicitly in their paper. The transformations between the homothetic and Schwarzschild coordinates and between the homothetic and comoving coordinates are given explicitly in Appendix B of Ref. [17], where the relationship between their variables and those of Ori and Piran [19], Maison [9] and Foglizzo and Henriksen [36] are also given. The relationsip between their variables and those used by Bogoyavenski [15] are given in Appendix B of Ref. [18].

Here we explicitly demonstrate the relationship between the variables used in this paper and those used in Foglizzo and Henriksen (FH) [36]. The main functions used in FH are the three quantities $(N,\ \overline{\mu},\ V^2)$, defined by Eqs. (FH3)–(FH5), which depend on the similarity variable $\xi \equiv z^{-1}$. The remaining self-similar functions can then be written in terms of these [see Eqs. (FH6)–(FH8)]. Their function V is identical to ours. Using Eqs. (2.12) and (FH3), we find that

$$N(z) = a_1 x^{(\alpha-1)/\alpha} z^{2(\alpha-1)/(1+\alpha)}, \tag{B1}$$

where a_1 is a constant. Using Eqs. (2.8), (2.12), (2.17) and (FH4), we obtain

$$\overline{\mu}(z) = 3\left[1 + (1+\alpha)\frac{\dot{S}}{S}\right]. \tag{B2}$$

Conversely, x and S can be defined explicitly in terms of $(N, \overline{\mu}, V^2)$ through Eq. (FH8),

$$S^2 = a_2 z^{(\alpha-1)/(1+\alpha)} [N|V|]^{-1}, \tag{B3}$$

and Eq. (B1), where a_2 is another constant.

The differential equations governing the evolution of $(N, \overline{\mu},\ V^2)$ are given by Eqs. (FH12)–(FH14); these constitute an autonomous system of ODEs in terms of the variable $\ln \xi = -\ln z$. Eqs. (FH12) and (FH13) are equivalent to our Eqs. (2.15) and (2.16). The first integral of the governing ODEs is given by Eq. (FH10) and is equivalent to our Eqs. (2.17) and (2.18). Equation (FH14), which governs the evolution of V^2, is obtained by differentiating V^2, defined by Eq. (2.19), and using the first integral. Consequently, the evolution equation (FH14) replaces Eqs. (2.17) and (2.18).

FH then regularize their system of equations by introducing a new independent variable, τ, defined by Eq. (FH15), which is equivalent to

$$\frac{d \ln z}{d\tau} = -1 + \alpha V^{-2}. \tag{B4}$$

This divides phase-space into two disconnected components. Although the resulting system of ODEs is autonomous, the system is not regular at $\xi = 0$ despite the fact that this point does not correspond to a physical singularity (i.e., it arises due to a coordinate problem at $\xi = 0$). FH then introduce new functions and coordinates so that solutions are completely regular at $(t=0, r>0)$. However, the resulting ODEs are no longer autonomous after this transformation.

APPENDIX C

The expansion of the comoving fluid velocity congruence, $\theta \equiv u^a{}_{;a}$, is given by

$$r\theta = z e^{-\nu} \Theta \tag{C1}$$

where

$$\Theta(z) \equiv -\frac{d}{dz}(\lambda + 2S) \tag{C2}$$

and λ is given by Eq. (2.1). When $p = \alpha\mu$, the conservation equations then yield

$$\frac{dW}{dz} = -(1+\alpha) W \Theta, \tag{C3}$$

where W is defined by Eq. (2.8). If we consider two comoving perfect fluids as the source of the gravitational field, each of which satisfies

$$p_i = \alpha_i \mu_i, \quad W_i = \mu_i R^2 \quad (\alpha = 1,2) \tag{C4}$$

(e.g., a mixture of dust and radiation with $\alpha_1 = 1/3$ and $\alpha_2 = 0$), then the source is equivalent to a single perfect fluid with

$$\mu = \mu_1 + \mu_2, \quad p = p_1 + p_2 = \alpha_1\mu_1 + \alpha_2\mu_2, \tag{C5}$$

although this does not admit an equation of state.

Suppose the two perfect fluids are non-interacting, with each separately satisfying the conservation equation (C3). Then

$$\frac{dW_i}{dz} = -(1+\alpha_i) W_i \Theta. \tag{C6}$$

We define a new variable

$$\chi = \chi(z) \equiv \frac{\mu_1 - \mu_2}{\mu_1 + \mu_2} = \frac{W_1 - W_2}{W_1 + W_2}, \tag{C7}$$

where $-1 \leqslant \chi \leqslant 1$. From Eq. (C6) we derive the evolution equation for χ:

$$\frac{d\chi}{d\tau} = \frac{1}{2}(\alpha_1 - \alpha_2)(1 - \chi^2) \tag{C8}$$

where τ is defined by

$$\frac{d\tau}{dz} = -\Theta \tag{C9}$$

for regions in which Θ (and hence the expansion θ) is nonzero.

Equation (C8) is a decoupled autonomous equation for χ. It has equilibrium points at $\chi=\pm 1$, and hence all solutions asymptote to $\chi=\pm 1$ in regions for which the expansion does not become zero. $\chi=+1$ corresponds to $\mu_2=0$ and $\chi=-1$ to $\mu_1=0$; i.e., these self-similar two-fluid solutions asymptote towards the exact asymptotes of the single perfect fluid solutions. Asymptotically $p/\mu\rightarrow\alpha_i$ and which value of α_i is picked out (i.e., which of the two single fluids govern the dynamics asymptotically) depends on the signs of $(\alpha_1-\alpha_2)$ and Θ and on whether $|z|\rightarrow 0$ or $|z|\rightarrow\infty$.

[1] M. E. Cahill and A. H. Taub, Commun. Math. Phys. **21**, 1 (1971).
[2] A. A. Coley and B. O. J. Tupper, J. Math. Phys. **30**, 2616 (1989).
[3] G. I. Barenblatt and Ya B. Zeldovich, Annu. Rev. Fluid Mech. **4**, 284 (1972).
[4] L. I. Sedov, *Similarity and Dimensional Methods in Mechanics* (Academic, New York, 1967).
[5] J. Schwartz, J. P. Ostriker, and A. Yahil, Astrophys. J. **202**, 1 (1975); S. Ikeuchi, K. Tomisaka, and J. Ostriker, *ibid.* **265**, 583 (1983).
[6] E. Bertschinger, Astrophys. J. **268**, 17 (1985).
[7] R. B. Larson, Mon. Not. R. Astron. Soc. **145**, 271 (1969); M. V. Penston, *ibid.* **144**, 449 (1969).
[8] M. W. Choptuik, Phys. Rev. Lett. **70**, 9 (1993); C. R. Evans, and J. S. Coleman, *ibid.* **72**, 1782 (1994); C. Gundlach, *ibid.* **75**, 3214 (1995); T. Koike, T. Hara, and S. Adachi, *ibid.* **74**, 5170 (1995); D. W. Neilsen and M. W. Choptuik, report, 1999.
[9] D. Maison, Phys. Lett. B **366**, 82 (1996).
[10] B. J. Carr, A. A. Coley, M. Goliath, U.S. Nilsson, and C. Uggla, report, 1999; Phys. Rev. D **61**, 081502(R) (2000).
[11] B. J. Carr, report prepared for but omitted from *The Origin of Structure in the Universe*, edited by E. Gunzig and P. Nardone (Kluwer, Dordrecht, 1993).
[12] J. Wainwright and G. F. R. Ellis, *Dynamical Systems in Cosmology* (Cambridge University Press, Cambridge, England, 1997).
[13] B. J. Carr, preceding paper, Phys. Rev. D **62**, 044022 (2000).
[14] O. I. Bogoyavlenski, Zh. Eksp. Teor. Fiz. **73**, 1201 (1977) [Sov. Phys. JETP **46**, 633 (1977)].
[15] O. I. Bogoyavlenski, *Methods in the Qualitative Theory of Dynamical Systems in Astrophysics and Gas Dynamics* (Springer-Verlag, Berlin, 1985).
[16] P. R. Brady, Class. Quantum Grav. **11**, 1254 (1994).
[17] M. Goliath, U. S. Nilsson, and C. Uggla, Class. Quantum Grav. **15**, 167 (1998).
[18] M. Goliath, U. S. Nilsson, and C. Uggla, Class. Quantum Grav. **15**, 2841 (1998).
[19] A. Ori and T. Piran, Phys. Rev. D **42**, 1068 (1990).
[20] B. J. Carr and A. A. Coley, Class. Quantum Grav. (to be published).
[21] A. A. Coley, in *Proceedings of the Sixth Canadian Conference on General Relativity and Relativistic Astrophysics*, The Fields Institute Communications Series (AMS), Vol. 15, edited by S. P. Braham, J. D. Gegenberg, and R. J. McKellar (AMS, Providence, RI, 1997).
[22] B. J. Carr, in *Proceedings of the Seventh Canadian Conference on General Relativity and Relativistic Astrophysics*, edited by D. Hobill (University of Calgary Press, Calgary, 1998).
[23] B. J. Carr and A. A. Coley, Class. Quantum Grav. **16**, R31 (1999).
[24] B. J. Carr and S. W. Hawking, Mon. Not. R. Astron. Soc. **168**, 399 (1974).
[25] B.J. Carr, Ph.D. thesis, Cambridge, 1976.
[26] G. V. Bicknell and R. N. Henriksen, Astrophys. J. **219**, 1043 (1978).
[27] D. N. C. Lin, B. J. Carr, and S. D. M. Fall, Mon. Not. R. Astron. Soc. **177**, 151 (1978).
[28] G. V. Bicknell and R. N. Henriksen, Astrophys. J. **225**, 237 (1978).
[29] B. J. Carr and A. Yahil, Astrophys. J. **360**, 330 (1990).
[30] B. J. Carr and A. Whinnett, report, 1999.
[31] R. Kantowski and R. Sachs, J. Math. Phys. **7**, 443 (1966).
[32] C. B. Collins, J. Math. Phys. **18**, 2116 (1977).
[33] B. J. Carr and A. Koutras, Astrophys. J. **405**, 34 (1993).
[34] P. Wesson, Phys. Rev. D **34**, 3925 (1986); Astrophys. J. **336**, 58 (1989); J. Ponce de Leon, J. Math. Phys. **29**, 2479 (1988); **31**, 371 (1990).
[35] C. W. Misner and H. S. Zapolsky, Phys. Rev. Lett. **12**, 634 (1964).
[36] T. Foglizzo and R. N. Henriksen, Phys. Rev. D **48**, 4645 (1993).
[37] R. N. Henriksen and K. Patel, Phys. Rev. D **42**, 1068 (1990); K. Lake, Phys. Rev. Lett. **68**, 3129 (1992); P. S. Joshi and I. H. Dwivedi, Phys. Rev. D **47**, 5357 (1993).
[38] R. N. Henriksen and P. S. Wesson, Astrophys. Space Sci. **53**, 429 (1978).
[39] B. D. Miller, Astrophys. J. **208**, 274 (1976).
[40] A. Whitworth and D. Summers, Mon. Not. R. Astron. Soc. **214**, 1 (1985).
[41] A. Ori and T. Piran, Mon. Not. R. Astron. Soc. **234**, 821 (1988).
[42] B. J. Carr and R. N. Henriksen, report, 2000.
[43] B. Carter and R. N. Henriksen, Ann. Phys. Supp. **14**, 47 (1989).
[44] P. M. Benoit and A.A. Coley, Class. Quantum Grav. **15**, 2397 (1998).
[45] A. A. Coley, Class. Quantum Grav. **8**, 954 (1991).
[46] J. Ponce de Leon, Gen. Relativ. Gravit. **25**, 865 (1993).
[47] A. V. Frolov, Phys. Rev. D **56**, 6433 (1997).
[48] R. N. Henriksen, A. G. Emslie, and P. S. Wesson, Phys. Rev. D **47**, 1219 (1993).
[49] U. S. Nilsson and C. Uggla, Class. Quantum Grav. **14**, 1964 (1997).